

1 Extending a land-surface model with Sphagnum moss to simulate responses of a northern  
2 temperate bog to whole-ecosystem warming and elevated CO<sub>2</sub>

3  
4 Xiaoying Shi<sup>1\*</sup>, Daniel M. Ricciuto<sup>1</sup>, Peter E. Thornton<sup>1</sup>, Xiaofeng Xu<sup>2</sup>, Fengming Yuan<sup>1</sup>,  
5 Richard J. Norby<sup>1</sup>, Anthony P. Walker<sup>1</sup>, Jeffrey Warren<sup>1</sup>, Jiafu Mao<sup>1</sup>, Paul J. Hanson<sup>1</sup>,  
6 Lin Meng<sup>3</sup>, David Weston<sup>1</sup>, Natalie A. Griffiths<sup>1</sup>

7 <sup>1</sup>Climate Change Science Institute and Environmental Sciences Division, Oak Ridge  
8 National Laboratory, Oak Ridge, TN 37831, USA

9 <sup>2</sup>Biology Department San Diego State University, San Diego, CA, 92182-4614, USA

10  
11 <sup>3</sup>Department of Geological and Atmospheric Sciences, Iowa State University, Ames, IA,  
12 50011

13  
14  
15 \* To whom correspondence should be addressed

16 Corresponding author's email: [shix@ornl.gov](mailto:shix@ornl.gov)

17 Fax: 865-574-2232

18

19  
20  
21  
22  
23  
24  
25  
26  
27  
28  
29  
30  
31  
32  
33  
34  
35  
36  
37  
38  
39

Formatted: Section start: Continuous

Formatted: Subscript

Formatted: Font: 10.5 pt

Deleted: Modeling the hydrology and physiology of *Sphagnum* moss in a northern temperate bog

42 **Abstract**

43

44

Mosses need to be incorporated into Earth system models to better simulate peatland functional dynamics under changing environment. *Sphagnum* mosses are strong determinants of nutrient, carbon and water cycling in peatland ecosystems. However, most land surface models do not include *Sphagnum* or other mosses as represented plant functional types (PFTs), thereby limiting predictive assessment of peatland responses to environmental change. In this study, we introduce a moss PFT into the land model component (ELM) of the Energy Exascale Earth System Model (E3SM), by developing water content dynamics and non-vascular photosynthetic processes for moss. The model was parameterized and independently evaluated against observations from an ombrotrophic forested bog as part of the Spruce and Peatland Responses Under Changing Environments (SPRUCE) project. Inclusion of a *Sphagnum* PFT with some *Sphagnum* specific processes in ELM allows it to capture the observed seasonal dynamics of *Sphagnum* gross primary production (GPP), albeit with an underestimate of peak GPP. The model simulated a reasonable annual net primary production (NPP) for moss but with less interannual variation than observed, and reproduced above ground biomass for tree PFTs and stem biomass for shrubs. Different species showed highly variable warming responses under both ambient and elevated atmospheric CO<sub>2</sub> concentrations, and elevated CO<sub>2</sub> altered the warming response direction for the peatland ecosystem. Microtopography is critical: *Sphagnum* mosses on hummocks and hollows were simulated to show opposite warming responses (NPP decreasing with warming on hummocks, but increasing in hollows), and hummock *Sphagnum* was modeled to have strong dependence on water table height. Inclusion of this new moss PFT in global ELM

66 simulations may provide a useful foundation for the investigation of northern peatland  
67 carbon exchange, enhancing the predictive capacity of carbon dynamics across the  
68 regional and global scales.

69 **Copyright statement**

70 This manuscript has been authored by UT-Battelle, LLC under Contract No. DE-  
71 AC05-00OR22725 with the U.S. Department of Energy. The United States Government  
72 retains and the publisher, by accepting the article for publication, acknowledges that the  
73 United States Government retains a non-exclusive, paid-up, irrevocable, world-wide  
74 license to publish or reproduce the published form of this manuscript, or allow others to  
75 do so, for United States Government purposes. The Department of Energy will provide  
76 public access to these results of federally sponsored research in accordance with the DOE  
77 Public Access Plan (<http://energy.gov/downloads/doe-public-access-plan>).

78  
79 **1. Introduction**

80 Boreal peatlands store at least 500 Pg of soil carbon due to incomplete  
81 decomposition of plant litter inputs resulting from a combination of low temperature and  
82 water-saturated soils. Because of this capacity to store carbon, boreal peatlands have  
83 played a critical role in regulating the global climate since the onset of the Holocene  
84 (Frolking and Roulet, 2007; Yu et al., 2010). The total carbon stock is large but  
85 uncertain: a new estimation of northern peatlands carbon stock of 1055 Pg was recently  
86 reported by Nichols and Peteet (2019). The rapidly changing climate at high latitudes is  
87 likely to impact both primary production and decomposition rates in peatlands,  
88 contributing to uncertainty in whether peatlands will continue their function as net carbon  
89

90 sinks in the long term (Moore et al., 1998; Turetsky et al., 2002; Wu and Roulet, 2014).  
91 Manipulative experiments and process-based models are thus needed to make defensible  
92 projections of net carbon balance of northern peatlands under anticipated global warming  
93 (Hanson et al, 2017; Shi et al., 2015).

94 Peatlands are characterized by a ground layer of bryophytes, and the raised or  
95 ombrotrophic bogs of the boreal zone are generally dominated by *Sphagnum* mosses that  
96 contribute significantly to total ecosystem CO<sub>2</sub> flux (Oechel and Van Cleve, 1986;  
97 Williams and Flanagan, 1998; Robroek et al., 2009; Vitt, 2014). *Sphagnum* mosses also  
98 strongly affect the hydrological and hydrochemical conditions at the raised bog surface  
99 (Van, 1995; Van der Schaaf, 2002). As a result, microclimate and *Sphagnum* species  
100 interactions influence the variability of both carbon accumulation rates and water and  
101 exchanges within peatland and between peatland and atmosphere (Heijmans et al., 2004a,  
102 2004b; Rosenzweig et al., 2008; Brown et al., 2010; Petrone et al., 2011; Goetz and Price,  
103 2015). Functioning as keystone species of boreal peatlands, *Sphagnum* mosses strongly  
104 influence the nutrient, carbon and water cycles of peatland ecosystems (Nilsson and  
105 Wardle, 2005; Cornelissen et al., 2007; Lindo and Gonzalez, 2010; Turetsky et al., 2010;  
106 Turetsky et al., 2012), and exert a substantial impact on ecosystem net carbon balance  
107 (Clymo and Hayward; 1982; Gorham, 1991; Wieder, 2006; Weston et al., 2015; Walker  
108 et al., 2017; Griffiths et al., 2018).

109 Numerical models are useful tools to identify knowledge gaps, examine long-term  
110 dynamics, and predict future changes. Earth system models (ESMs) simulate global  
111 processes, including the carbon cycle, and are primarily used to make future climate  
112 projections. Poor model representation of carbon processes in peatlands is identified as a

Deleted: water exchanges between and within peatlands

114 deficiency causing biases in simulated soil organic mass and heterotrophic respiratory  
115 fluxes for current ESMs (Todd-Brown et al., 2013; Tian et al., 2015). Although most  
116 ESMs do not include moss, a number of offline dynamic vegetation models and  
117 ecosystem models do include one or more moss plant functional types (PFTs) (Pastor et  
118 al., 2002; Nungesser, 2003; Zhuang et al., 2006; Bond-Lamberty et al., 2007; Heijmans et  
119 al., 2008; Euskirchen et al., 2009; Wania et al., 2009; Frolking et al., 2010). Several  
120 peatland-specific models contain moss species and have been applied globally or at  
121 selected peatland sites. For example, the McGill Wetland Model (MWM) was evaluated  
122 using the measurements at Degerö Stormyr and the Mer Bleue bogs (St-Hilaire et al.,  
123 2010). The peatland version of the General Ecosystem Simulator - Model of Raw Humus,  
124 Moder and Mull (GUESS-ROMUL) was used to simulate the changes of daily CO<sub>2</sub>  
125 exchange rates with water table position at a fen (Yurova et al., 2007). The PEATBOG  
126 model was implemented to characterize peatland carbon and nitrogen cycles in the Mer  
127 Bleue bog, including moss PFTs but without accounting for microtopography (Wu et al.,  
128 2013a). The CLASS-CTEM model (the coupled Canadian Land Surface Scheme and the  
129 Canadian Terrestrial Ecosystem Model), which includes a moss layer as the first soil  
130 layer, was applied to simulate water, energy and carbon fluxes at eight different peatland  
131 sites (Wu et al., 2016). The IAP-RAS (Institute of Applied Physics – Russian Academy  
132 of Sciences) wetland methane (CH<sub>4</sub>) model with a 10 cm thick moss layer (Mokhov et al.  
133 2007) was run globally to simulate the distribution of CH<sub>4</sub> fluxes (Wania et al., 2013).  
134 The CHANGE model (a coupled hydrological and biogeochemical process simulator),  
135 which includes a moss cover layer (Launiainen et al., 2015), was used to investigate the  
136 effect of moss on soil temperature and carbon flux at a tundra site in Northeastern Siberia

137 (Park et al., 2018). [Chadburn et al. \(2015\)](#) added a surface layer of moss to JULES land  
138 [surface model to consider the insulating effects and treated the thermal conductivity of](#)  
139 [moss depending on its water content to investigate the permafrost dynamics.](#) [Porada et al.](#)  
140 [\(2016\)](#) integrated a stand-alone dynamic non-vascular vegetation model LiBry ([Porada et](#)  
141 [al., 2013](#)) to land surface scheme JSBACH, but JSBACH mainly represent bryophyte and  
142 [lichen cover on upland forest, not for peatland ecosystem without including an organic](#)  
143 [soil layer.](#) [Druel et al. \(2017\)](#) investigated the vegetation-climate feedbacks in high  
144 [latitudes by introducing a non-vascular plant type representing mosses and lichens to the](#)  
145 [global land surface model ORCHIFEE.](#) Moreover, those models did not consider  
146 [microtopography and the lateral transports between hummocks and hollows.](#) Two  
147 models, the “ecosys” model ([Grant et al., 2012](#)) and CLM\_SPRUCE ([Shi et al., 2015](#)),  
148 have been parameterized to represent peatland microtopographic variability (e.g., the  
149 hummock and hollow microterrain characteristic of raised bogs) with lateral connections  
150 across the topography. Prediction of water table dynamics in the “ecosys” model is  
151 constrained by specifying a regional water table at a fixed height and a fixed distance  
152 from the site of interest, thereby missing key controlling factors of a precipitation-driven  
153 dynamic water table ([Shi et al., 2015](#)). The CLM\_SPRUCE model ([Shi et al., 2015](#)) was  
154 developed to parameterize the hydrological dynamics of lateral transport for  
155 microtopography of hummocks and hollows in the raised bog environment of the  
156 SPRUCE (Spruce and Peatland Responses Under Changing Environments) experiment  
157 ([Hanson et al., 2017](#)). That model version did not include the biophysical dynamics of  
158 *Sphagnum* moss, and used a prescribed leaf area instead of allowing leaf area to evolve  
159 prognostically.

160 \_\_\_\_ In this study, we introduce a new *Sphagnum* moss PFT into the model, and migrate  
161 the entire raised-bog capability into the new Energy Exascale Earth System Model  
162 (E3SM), specifically into version 1 of the E3SM land model (ELM v1, Ricciuto et al.,  
163 2018). The objectives of this study are to: 1) introduce a *Sphagnum* PFT to the ELM  
164 model with additional *Sphagnum*-specific processes to better capture the peatland  
165 ecosystem; and 2) apply the updated ELM to explore how an ombrotrophic, raised-dome  
166 bog peatland ecosystem will respond to different scenarios of warming and elevated  
167 atmospheric CO<sub>2</sub> concentration.

## 168 2. Model description

### 169 2.1 Model provenance

170 ELM v1 is the land component of E3SM v1, which is supported by the US  
171 Department of Energy (DOE). Developed by multiple DOE laboratories, E3SM consists  
172 of atmosphere, land, ocean, sea ice, and land ice components, linked through a coupler  
173 that facilitates across-component communication (Golaz et al., 2019). ELM was  
174 originally branched from the Community Land Model (CLM4.5, Oleson et al., 2013),  
175 with new developments that include representation of coupled carbon, nitrogen, and  
176 phosphorus controls on soil and vegetation processes, and new plant carbon and nutrient  
177 storage pools (Ricciuto et al., 2018; Yang et al., 2019; Burrows et al., 2020). Inputs of  
178 new mineral nitrogen of ELM are from atmospheric deposition and biological nitrogen  
179 fixation. The fixation of new reactive nitrogen from atmospheric N<sub>2</sub> by soil  
180 microorganisms is an important component of nitrogen budgets. ELM follows the  
181 approach of Cleveland et al. (1999) that uses an empirical relationship of biological

Formatted: Normal (Web), Tab stops: Not at 0.5"

Formatted: Font: (Default) Times New Roman, 12 pt

Deleted: in review

Formatted: Font: (Default) Times New Roman, 12 pt

Formatted: Font: (Default) Times New Roman, 12 pt, Subscript, Not Raised by / Lowered by

Formatted: Font: (Default) Times New Roman, 12 pt, Not Raised by / Lowered by

Formatted: Font: (Default) Times New Roman, 12 pt

Formatted: Font: (Default) Times New Roman, 12 pt, Font color: Auto

Formatted: Font: (Default) Times New Roman, 12 pt, Font color: Auto

183 nitrogen fixation as a function of net primary production to predict the nitrogen fixation,  
184 The model version used in this study is designated ELM SPRUCE, and includes the new  
185 implementation of Sphagnum mosses as well as the hydrological dynamics of lateral  
186 transport between hummock and hollow microtopographies. The implementation has  
187 been parameterized based on observations from the S1-Bog in northern Minnesota, USA,  
188 as described by Shi et al. (2015), with additional details provided below.

Formatted: Font: (Default) Times New Roman, 12 pt

Deleted: \_

Formatted: Font: Times New Roman, 12 pt, Not Italic

Formatted: Font: (Default) Times New Roman, 12 pt

Formatted: Font: (Default) Times New Roman, 12 pt

## 189 2.2 Non-vascular plants: *Sphagnum* mosses

Formatted: Font: Italic

190 To represent non-vascular plant the *Sphagnum* mosses, we modified the C3 artic  
191 grasses equations as follows. We considered *Sphagnum* biomass to be represented mainly  
192 by leaf and stem carbon (only a very shallow root). In addition, we modified the vascular  
193 C3 arctic grasses equations for photosynthesis and stomatal conductance (see the below  
194 new model development), and the associated parameters as reported by Table 1-3. We  
195 use the same framework as for C3 arctic grasses, but the Ball-Berry slope term is assumed  
196 to be zero and the intercept term is the conductance term as a function of water content of  
197 *Sphagnum* mosses. For all other processes like the evapo(transpi)ration and associated  
198 parameters not described below, we used the C3 arctic grasses equations (reported by  
199 Oleson et al., 2013). Drying impacts the conductance and affects evapo(transpi)ration of  
200 the internal water. The SLA and leaf C:N ratio parameters are strong controls on  $V_{cmax}$ ,  
201 and therefore overall productivity and *Sphagnum* moss LAI. The high sensitivities occur  
202 because LAI is a strong control on evapo(transp)iration.

Formatted: Font: Not Italic

Formatted: Left, Tab stops: Not at 0.5"

Formatted: Font: Not Italic

Formatted: Font: Times New Roman

Formatted: Font: Times New Roman, Italic

Formatted: Font: Times New Roman

Formatted: Font: Times New Roman

Formatted: Font: Times New Roman

Formatted: Font: Times New Roman, 12 pt, Not Raised by / Lowered by

Formatted: Font: Times New Roman

## 203 2.3 New model developments

Deleted: ¶

Deleted: 2

### 204 2.3.1 Water content dynamics of *Sphagnum* mosses

Deleted: 2



209 The main sources for water content of *Sphagnum* mosses are passive capillary  
210 water uptake from peat, and interception of atmospheric water on the capitulum (growing  
211 tip of the moss) (Robroek et al. 2007). Capillary water uptake, the internal *Sphagnum*  
212 moss water content, is modeled as functions of soil water content and evaporation losses.  
213 Water intercepted on the *Sphagnum* moss capitulum is modeled as a function of moss  
214 foliar biomass, current canopy water, water drip, and evaporation losses.

215 ~~Since evaporation at the *Sphagnum* surface depends on atmospheric water vapor~~  
216 ~~deficit, moss-atmosphere conductance and available water pool which depends on~~  
217 ~~capillary wicking of water up to the surface.~~ At SPRUCE, the peat volumetric water  
218 content is measured at several depths using automated sensors (model 10HS, Decagon  
219 Devices, Inc., Pullman, WA) calibrated for the site-specific upper peat soil using  
220 mesocosms (reference Figure S1, Hanson et al. 2017). ~~During those calibrations, we~~  
221 periodically sampled the surface *Sphagnum* for gravimetric water content and water  
222 potential using a dew point potentiometer (WP4, Decagon Devices, Inc.), which also  
223 provided a surface soil water retention curve. The destructive sampling of surface  
224 *Sphagnum* was primarily hummock species but did included some hollow species. The  
225 automated measurements of peat water content at 10 cm depth were shown to be a good  
226 indicator of surface *Sphagnum* water content (Fig. 1). Based on this relationship, we  
227 model the water content of *Sphagnum* moss due to capillary rise ( $W_{internal}$ ) (g water /g  
228 dry moss) as:

$$229 W_{internal} = 0.3933 + 7.6227 / (1 + \exp(-(\text{Soil}_{vol} - 0.1571))) / 0.018 \quad (1)$$

230 where  $\text{Soil}_{vol}$  is the averaged volumetric soil water of modeled soil layers nearest the  
231 10cm depth horizon (layers 3 and 4 in the ELM v1 vertical layering scheme).

Formatted: Font: Italic

Deleted: Since evaporation at the *Sphagnum* surface depends on capillary wicking of water up to the surface and atmospheric water vapor deficit, we developed a relationship between measured soil water content at depth, and surface *Sphagnum* water content

Deleted: W

Deleted: .

239 The *Sphagnum* moss surface water ( $W_{surface}$ ) was calculated using the model  
 240 predicted canopy water and the dry foliar biomass as:

$$241 \quad W_{surface} = can\_water / fmass \quad (2)$$

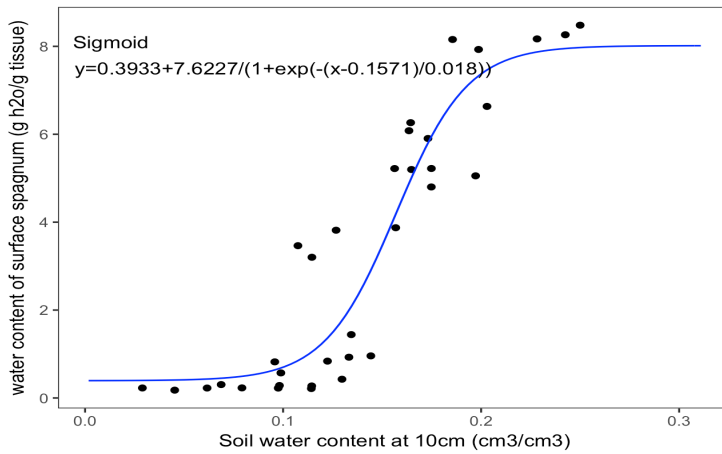
242 where  $W_{surface}$  (g water /g dry moss) is the surface water content and  $fmass$  is the foliar  
 243 biomass of *Sphagnum* mosses. The  $can\_water$  is the *Sphagnum* moss canopy water and it  
 244 is simulated by a function of interception, canopy drip, dew and canopy evaporation  
 245 (Oleson et al., 2013).

Deleted: opy

246 The total water content ( $W_{total}$ ) of *Sphagnum* mosses is the sum of water taken  
 247 up from peat and the surface water content (St-Hilaire et al, 2010; Wu et al., 2013).

$$248 \quad W_{total} = W_{internal} + W_{surface} \quad (3)$$

249



250  
 251 Figure 1. The measured relationship between soil water content at depth and the water content of  
 252 surface *Sphagnum* based on destructive sampling.  
 253

### 2.3.2 Modeling *Sphagnum* CO<sub>2</sub> conductance and photosynthesis

ELM\_SPRUCE computes photosynthetic carbon uptake (gross primary production, or GPP) for each vascular PFT on a half-hourly time step, based on the Farquhar biochemical approach (Farquhar et al., 1980; Collatz et al., 1991, 1992), with implementation as described by Oleson et al. (2013). While, *Sphagnum* lacks a leaf cuticle and stomata that regulate water loss and CO<sub>2</sub> uptake in vascular plants (Titus et al. 1983). The primary transport pathway for CO<sub>2</sub> is through the cells and is analogous to mesophyll conductance in higher plants. Thus, we calculate the total conductance to CO<sub>2</sub> for *Sphagnum* mosses by using total water content following the method reported by Williams and Flanagan (1998) described as below. Goetz and Price (2015) also indicated that capillary rise through the peat is essential to maintain a water content sufficient for photosynthesis for *Sphagnum* moss species, but that atmospheric inputs can provide small but critical amounts of water for physiological processes.

The stomatal conductance for vascular plant types in ELM\_SPRUCE is derived from the Ball-Berry conductance model (Collatz et al., 1991). That model relates stomatal conductance to net leaf photosynthesis, scaled by the relative humidity and the CO<sub>2</sub> concentration at the leaf surface. The stomatal conductance ( $g_s$ ) and boundary layer conductance ( $g_b$ ) are required to obtain the internal leaf CO<sub>2</sub> partial pressure ( $C_i$ ) of vascular PFTs:

$$C_i = C_a - \left( \frac{1.4g_s + 1.6g_b}{g_s g_b} \right) P_{atm} A_n \quad (4)$$

where  $C_i$  is the internal leaf CO<sub>2</sub> partial pressure,  $C_a$  is the atmospheric CO<sub>2</sub> partial

Deleted: 2

Formatted: Font: Italic

Formatted: Not Superscript/ Subscript

**Deleted:** The internal water content of *Sphagnum* mosses is observed to affect photosynthesis by constraining the length of the diffusive path for CO<sub>2</sub> through the variably-hydrated external hyaline cells to the carbon fixation sites (Robroek et al., 2009; Rydin and Jeglum, 2006). Goetz and Price (2015) also indicated that capillary rise through the peat is essential to maintain a water content sufficient for photosynthesis for *Sphagnum* moss species, but that atmospheric inputs can provide small but critical amounts of water for physiological processes. *Sphagnum* lacks a leaf cuticle and stomata that regulate water loss and CO<sub>2</sub> uptake in vascular plants (Titus et al. 1983). The primary transport pathway for CO<sub>2</sub> is through the cells and is analogous to mesophyll conductance in higher plants.

291 pressure,  $A_n$  is leaf net photosynthesis ( $\mu \text{ mol CO}_2 \text{ m}^{-2} \text{ s}^{-1}$ )  $P_{atm}$  is the atmospheric  
292 pressure,  $g_s$  is the leaf stomatal conductance,  $g_b$  is the leaf boundary layer conductance,  
293 and values 1.4 and 1.6 are the ratios of the diffusivity of  $\text{CO}_2$  to  $\text{H}_2\text{O}$  for stomatal  
294 conductance and the leaf boundary layer conductance, respectively.

295 For *Sphagnum* moss photosynthesis, we followed the method from the McGill  
296 Wetland Model (St-Hilaire et al. 2010; Wu et al., 2013), which is based on the effects of  
297 *Sphagnum* moss water content on photosynthetic capacity (Tenhunen et al., 1976) and  
298 total conductance of  $\text{CO}_2$  (Williams and Flanagan, 1998), and replaces the stomatal  
299 conductance representation used for vascular PFTs.

$$300 \quad C_i = C_a - \frac{P_{atm} A_n}{g_{tc}} \quad (5)$$

301 The total conductance to  $\text{CO}_2$  ( $g_{tc}$ ) was determined from a least-squares regression  
302 described by Williams and Flanagan (1998) as:

$$303 \quad g_{tc} = -0.195 + 0.134W_{total} - 0.0256W_{total}^2 + 0.0028W_{total}^3 - \\ 304 \quad 0.0000984W_{total}^4 + 0.00000168W_{total}^5 \quad (6)$$

305 where  $W_{total}$  is as defined in equation (3). This relationship is only valid up to the  
306 maximum water holding capacity of mosses. To be noted that we assume that the  
307 boundary layer conductance is greater than moss surface layer conductance, and the moss  
308 surface layer conductance is greater than chloroplast conductance.

309 In addition to the water content, the effects of moss submergence were taken into  
310 account in the calculation of moss photosynthesis. Walker et al. (2017) reported

Formatted: Font: Italic

311 significant impacts of submergence on measured *Sphagnum* GPP and modeled the effect  
312 by modifying the *Sphagnum* leaf (stem) area index. Submergence in Walker et al. (2017) was  
313 expressed as photosynthesising stem area index (SAI) as a logistic function of water table depth.  
314 A maximum SAI of 3 was used and the parameter combination that most closely described the  
315 GPP data gave a range of water table depth from -10 cm for complete submergence and SAI of  
316 ~2.5 at 10 cm. This allowed for a range of processes such as floatation of *Sphagnum* with the  
317 water table, and adhesion of water to the *Sphagnum* capitula. For simplicity, in  
318 ELM\_SPRUCE, we calculated such impacts on *Sphagnum* GPP directly as a function of  
319 the height of simulated surface water, assuming that GPP from the submerged portion of  
320 photosynthetic tissue is negligible. GPP is thus reduced linearly according to the  
321 following equation:

$$322 \text{GPP}_{\text{sub}} = \text{GPP}_{\text{orig}} * (h_{\text{moss}} - \text{H}_2\text{O}_{\text{sfc}}) \quad (7)$$

323 where  $\text{GPP}_{\text{sub}}$  is the GPP corrected for submergence effects,  $\text{GPP}_{\text{orig}}$  is the original GPP,  
324  $\text{H}_2\text{O}_{\text{sfc}}$  is the surface water height, and  $h_{\text{moss}}$  is the height of the photosynthesizing  
325 *Sphagnum* layer above the soil surface, set to 5cm in our simulations. If  $\text{H}_2\text{O}_{\text{sfc}}$  is equal to  
326 or greater than  $h_{\text{moss}}$ , GPP is reduced to zero. Because in our simulations surface water is  
327 never predicted to occur in the hummocks, in practice this submergence effect only  
328 affects the moss GPP in the hollows.

### 329 **3. Methods**

#### 330 **3.1 Site Description**

331 We focused on a high C, ombrotrophic peatland (the S1-Bog) that has a perched  
332 water table with limited groundwater influence (Sebestyen et al. 2011, Griffiths and  
333 Sebestyen, 2016). This southern boreal bog is located on the Marcell Experimental

Formatted: Font: Italic

Formatted: Font: Italic

334 Forest, approximately 40 km north of Grand Rapids, Minnesota, USA (47.50283 degrees  
335 latitude, -93.48283 degrees longitude) (Sebestyen et al. 2011), and is the site of the  
336 SPRUCE climate change experiment (<http://mnspruce.ornl.gov>; Hanson et al., 2017). The  
337 S1-Bog has a raised hummock and sunken hollow microtopography, and it is nearly  
338 covered by *Sphagnum* mosses. *S. angustifolium* (C.E.O. Jensen ex Russow) and *S. fallax*  
339 (Klinggr.) occupy 68% of the moss layer and exist in both hummocks and hollows. *S.*  
340 *magellanicum* (Brid.) occupies ~20% of the moss layer and is primarily limited to the  
341 hummocks (Norby et al., 2019). The vascular plant community at the S1-Bog is  
342 dominated by the evergreen tree *Picea mariana* (Mill.) B.S.P, the deciduous tree *Larix*  
343 *laricina* (Du Roi) K. Koch, and a variety of ericaceous shrubs. Trees are present due to  
344 natural regeneration following strip cut harvesting in 1969 and 1974 (Sebestyen et al.,  
345 2011). The soil of this peat bog is the Greenwood series, a Typic Haplohemist  
346 (<https://websoilsurvey.sc.egov.usda.gov>), and its average peat depth is 2 to 3 m  
347 (Parsekian et al., 2012)

348 Northern Minnesota has a subhumid continental climate with average annual  
349 precipitation of 768 mm and annual air temperature of 3.3 °C for the time period from  
350 1965 to 2005. Mean annual air temperatures at the bog have increased about 0.4 °C per  
351 decade over the last 40 years (Verry et al., 2011).

### 352 3.2 Field measurements

353 Multiple observational pre-treatment data ([the data were collected prior to](#)  
354 [initiation of the warming and CO<sub>2</sub> treatments](#)) were used in this study. Flux-partitioned  
355 GPP of *Sphagnum* mosses was derived from measured hourly *Sphagnum*-peat net  
356 ecosystem exchange (NEE) flux (Walker et al., 2017). The GPP – NEE relationship was

Formatted: Subscript

357 also evaluated using observed vegetation growth and productivity allometric and biomass  
358 data on tree species, stem biomass for shrub species (Hanson et al., 2018a and b), and  
359 *Sphagnum* pre-treatment net primary productivity (NPP) (Norby et al., 2019).  
360 ELM\_SPRUCE was driven by climate data (temperature, precipitation, relative humidity,  
361 solar radiation, wind speed, pressure and long wave radiation) from 2011 to 2017  
362 measured at the SPRUCE S1-Bog (Hanson et al., 2015a and b). The surface weather  
363 station is outside of the enclosures and not impacted by the experimental warming  
364 treatments that began in 2015. These data are available at <https://mnspruce.ornl.gov/>.

### 365 366 **3.3 Simulation of the SPRUCE experiment**

367 Based on measurements at the SPRUCE site, ELM\_SPRUCE includes four  
368 PFTs: boreal evergreen needleleaf tree (*Picea*), boreal deciduous needleleaf tree (*Larix*),  
369 boreal deciduous shrub (representing several shrub species), and the newly introduced  
370 *Sphagnum* moss PFT. Currently ELM\_SPRUCE does not include light competition  
371 among multiple PFTs, and thus does not represent cross-PFT shading effects. Our model  
372 also allows the canopy density of PFTs to change prognostically, and their fractional  
373 coverage is held constant. We used measurements from *Sphagnum* moss collected at a  
374 tussock tundra site in Alaska (Hobbie 1996) to set several of the model leaf litter  
375 parameters for our simulations (Table 1). The values for other parameters have been  
376 optimized based on observations at the SPRUCE site (Table 2 and 3, optimization  
377 methods described in section 3.4). We prescribe both hummock and hollow  
378 <https://scratch.mit.edu/projects/411435898> microtopographies to have the same fractional  
379 PFT distribution. Consistent with Shi et al. (2015), hummocks and hollows were

380 modeled on separate columns with lateral flow of water between them. All the  
381 ELM\_SPRUCE simulations were conducted using a prognostic scheme for canopy  
382 phenology (Olesen et al., 2013).

383 The SPRUCE experiment at the S1-Bog consists of combined manipulations of  
384 temperature (various differentials up to +9 °C above ambient) and atmospheric CO<sub>2</sub>  
385 concentration (ambient and ambient + 500 ppm) applied in 12 m diameter x 8 m tall  
386 enclosures constructed in the S1-Bog. The whole-ecosystem warming began in August  
387 2015, elevated CO<sub>2</sub> started from June 2016, and various treatments are envisioned to  
388 continue until 2025. Extensive pre-treatment observations at the site began in 2009.

389 For the ELM\_SPRUCE, we continuously cycled the 2011-2017 climate forcing  
390 (see section 3.2) to equilibrate carbon and nitrogen pools under pre-industrial  
391 atmospheric CO<sub>2</sub> concentrations and nitrogen deposition, and then launched a simulation  
392 starting from year 1850 through year 2017. This transient simulation includes historically  
393 varying CO<sub>2</sub> concentrations, nitrogen deposition, and the land-use effects of a strip cut  
394 and harvest at the site in 1974. These simulations were used to compare model  
395 performance with pre-treatment observations. A subset of these observations was also  
396 used for optimization and calibration (section 3.4).

397 To investigate how the bog vegetation may respond to different warming  
398 scenarios and elevated atmospheric CO<sub>2</sub> concentrations, we performed 11 model runs  
399 from the same starting point in year 2015. These simulations were designed to reflect the  
400 warming treatments and CO<sub>2</sub> concentrations being implemented in the SPRUCE  
401 experiment enclosures. The model simulations include one ambient case (both ambient  
402 temperature and CO<sub>2</sub> concentration), and five simulations with modified input air



403 temperatures to represent the whole-ecosystem warming treatments at five levels (+0 °C,  
 404 +2.25 °C, +4.50 °C, +6.75 °C and +9.00 °C above ambient) and at ambient CO<sub>2</sub>, and  
 405 another five simulations with the same increasing temperature levels and at elevated CO<sub>2</sub>  
 406 (900 ppm). In the treatment simulations, we also considered the passive enclosure  
 407 effects, which reduce incoming shortwave and increase incoming longwave radiation  
 408 (Hanson et al., 2017). Following the SPRUCE experimental design, there was no water  
 409 vapor added so that the simulations used constant specific humidity instead of constant  
 410 relative humidity across the warming levels. All the treatment simulations were  
 411 performed through the year 2025 by continuing to cycle the 2011-2017 meteorological  
 412 inputs (with modified temperature and radiation to reflect the treatments) to simulate  
 413 future years.

414 Table 1: Physiological parameters of *Sphagnum* mosses as given in Hobbie 1996

Parameters	Description	Values
lf_liten	Leaf litter C:N ratio (gC/gN)	66
lf_fccl	Leaf litter fraction of cellulose	0.737
lf_flab	Leaf litter fraction of labile	0.227
lf_flg	Leaf litter fraction of lignin	0.036

415

### 416 3.4. Model sensitivity analysis and calibration

417 The vegetation physiology parameters in ELM\_SPRUCE were originally derived  
 418 from CLM4.5 and its predecessor, Biome-BGC, and represent broad aggregations of  
 419 plant traits over many species and varied environmental conditions (White et al., 2000).

420 To achieve reasonable model performance at SPRUCE, site-specific parameters and  
421 targeted parameter calibration are needed. Since the ELM\_SPRUCE contains over 100  
422 uncertain parameters, parameter optimization is not computationally feasible without first  
423 performing some dimensionality reduction. Based on previous ELM sensitivity analyses  
424 (e.g., Lu et al., 2018; Ricciuto et al., 2018; Griffiths et al., 2018), we chose 35 model  
425 parameters for further calibration (Tables 2 and 3). An ensemble of 3000 ELM\_SPRUCE  
426 simulations were conducted using the procedure described in 3.3, with each ensemble  
427 member using a randomly selected set of parameter values within uniform prior ranges.  
428 This model ensemble was first used to construct a polynomial chaos surrogate model,  
429 which was then used to perform a global sensitivity analysis (Sargsyan et al., 2014;  
430 Ricciuto et al., 2018). Main sensitivity indices, reflecting the proportion of output  
431 variance that occurs for each parameter, are described in section 4.1.

432 To minimize potential biases in model predictions of treatment responses, we  
433 calibrated the same 35 model parameters using pre-treatment observations as data  
434 constraints. We employed a quantum particle swarm optimization (QPSO) algorithm (Lu  
435 et al., 2018). While this method does not allow for the calculation of posterior prediction  
436 uncertainties, it is much more computationally efficient than other methods such as  
437 Markov Chain Monte Carlo. The constraining data included *year 2012-2013* tree growth  
438 and biomass (Hanson et al. 2018a), *year 2012-2013* shrub growth and biomass (Hanson  
439 et al., 2018b), *year 2012 and 2014 Sphagnum* net primary productivity (Norby et al.,  
440 2017, 2019), enclosure-averaged leaf area index by PFT (*year 2011 for tree and year*  
441 *2012 for shrub and Sphagnum*), and *year 2011-2013* water table depth (WTD)  
442 observations, aggregated to seasonal averages (Hanson et al., 2015b). The goal of the

Formatted: Font: Italic

443 optimization is to minimize a cost function, which we define here as a sum of squared  
 444 errors over all observation types weighted by observation uncertainties. When  
 445 observation uncertainties were not available, we assumed a range of  $\pm 25\%$  from the  
 446 default value. Site measurements were also used to constrain the ranges of two  
 447 parameters: *leafcn* (leaf carbon to nitrogen ratio) and *slatop* (specific leaf area at canopy  
 448 top). The uniform prior ranges for these parameters represent the range of plot to plot  
 449 variability. Optimized parameter values are shown in Table 2 and 3. Section 4 reports the  
 450 results of simulations using these optimized parameters, which were used to perform a  
 451 spinup, transient (1850-2017) and set of 11 treatment simulations (2015-2025) as  
 452 described above.

453 Table 2: PFT-specific optimized model parameters

Parameter	Description	<i>Sphagnum</i>	<i>Picea</i>	<i>Larix</i>	Shrub	Range
flnr	Rubisco-N fraction of leaf N	0.2906	0.0678	0.2349	0.2123	[0.05,0.30]
croot_stem	Coarse root to stem allocation ratio	N/A	0.2540	0.1529	0.7540	[0.05,0.8]
stem_leaf <sup>1</sup>	Stem to leaf allocation ratio	N/A	1.047	1.016	0.754	[0.3,2.2]
leaf_long	Leaf longevity (yr)	0.9744	5 <sup>3</sup>	N/A	N/A	[0.75, 2.0]
slatop	Specific leaf area at canopy top ( $\text{m}^2 \text{gC}^{-1}$ )	0.00781	0.00462	0.0128	0.0126	[0.004,0.04]
leafcn	Leaf C to N ratio	35.56	70.17	64.84	33.14	[20,75]
froot_leaf <sup>2</sup>	Fine root to leaf allocation ratio	0.3944	0.8567	0.3211	0.6862	[0.15, 2.0]
mp	Ball-Berry stomatal conductance slope	N/A	7.50	9.32	10.8	[4.5, 12]

454 Optimized values of PFT-specific parameters. The range column values in brackets indicate the range of  
 455 acceptable parameter values used in the sensitivity analysis and the optimization across all four PFTs in the  
 456 format [minimum, maximum]. N/A indicates that parameter is not relevant for that PFT.

457 <sup>1</sup>for tree PFTs, this parameter depends on NPP. The value shown is the allocation at an NPP of  $800 \text{ gC m}^{-2}$   
 458  $\text{yr}^{-1}$ .

459 <sup>2</sup> the fine root pool is used as a surrogate for non-photosynthetic tissue in *Sphagnum*

460 <sup>3</sup> This parameter was not optimized; we used the default value.

461

462

463 Table 3: Non PFT-specific optimized model parameters

	Description	Optimized value	Default	Range
r_mort	Vegetation mortality	0.0497	0.02	[0.005, 0.1]
decomp_depth_efolding	Depth-dependence e-folding depth for decomposition (m)	0.3899	0.5	[0.2, 0.7]
qdrai,0	Maximum subsurface drainage rate (kg m <sup>-2</sup> s <sup>-1</sup> )	3.896e-6	9.2e-6*	[0, 1e-3]
Q10_mr	Temperature sensitivity of maintenance respiration	2.212	1.5	[1.2, 3.0]
br_mr	Base rate for maintenance respiration (gC gN m <sup>2</sup> s <sup>-1</sup> )	4.110e-6	2.52e-6	[1e-6, 5e-6]
crit_onset_gdd	Critical growing degree days for leaf onset	99.43	200	[20, 500]
lw_top_ann	Live wood turnover proportion (yr <sup>-1</sup> )	0.3517	0.7	[0.2, 0.85]
gr_perc	Growth respiration fraction	0.1652	0.3	[0.12, 0.4]
rdrai,0	Coefficient for surface water runoff (kg m <sup>-4</sup> s <sup>-1</sup> )	6.978e-7	8.4e-8*	[1e-9, 1e-6]

464 Optimized and default values for non PFT-specific parameters. The range column values in brackets  
 465 indicate the range of acceptable parameter values used in the sensitivity analysis and the  
 466 optimization in the format [minimum, maximum].

467 \*Previously calibrated value from Shi et al (2015)

468

- Formatted: Font color: Text 1
- Formatted: Normal, No bullets or numbering
- Formatted: Font: 10 pt

## 469 4. Results

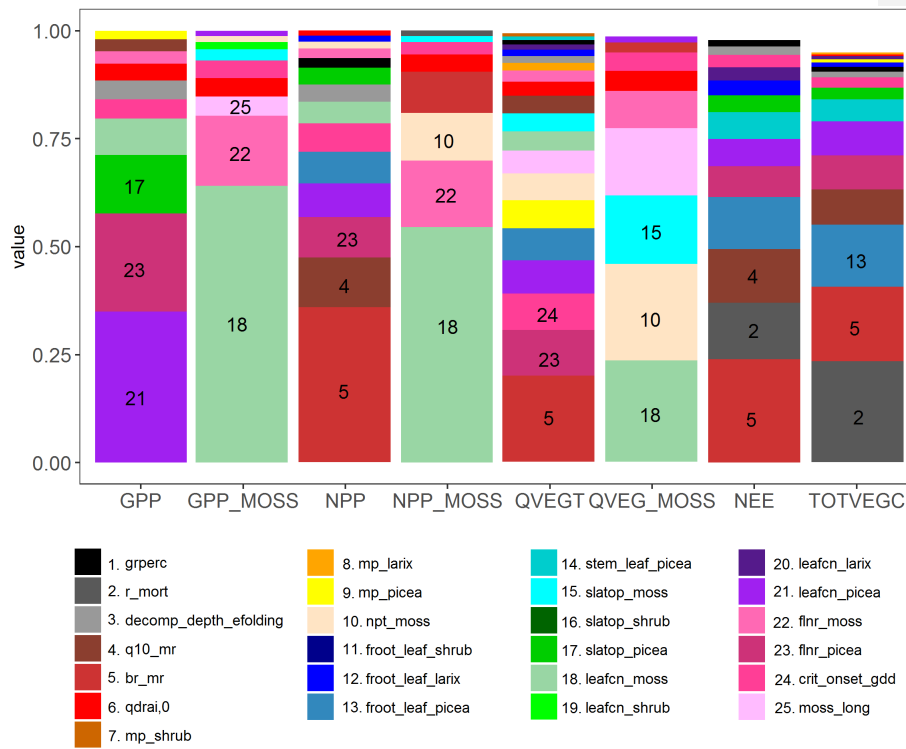
### 470 4.1 Model sensitivity analysis

471 Main effect (first-order) sensitivities are shown for eight model output quantities of  
 472 interest: Total site gross primary productivity (GPP), GPP for the moss PFT only  
 473 (GPP\_moss), total site net primary productivity (NPP), NPP for the moss PFT only  
 474 (NPP\_moss), total site vegetation transpiration (QVEGT), evaporation from the moss  
 475 surface (QVEG\_moss), net ecosystem exchange (NEE) and site total vegetation carbon

476 (TOTVEGC) (Fig. 2). Out of 35 parameters investigated, 25 show a sensitivity index of  
477 at least 0.01 for one of the quantities of interest, and these are plotted on figure 2. In that  
478 figure, sensitivities are stacked in order from highest to lowest for each variable, with the  
479 height of the bar equal to the sensitivity index. The first order sensitivities sum to at least  
480 0.95 for all variables, indicating that higher order sensitivities (i.e., contributions to the  
481 sensitivity from combinations of two or more parameters) contribute relatively little to  
482 the variance for these quantities of interest.

483         According to this analysis, the variance in total site GPP is dominated by three  
484 *Picea* parameters: the fraction of leaf nitrogen in RuBiCO (*flnr\_picea*), leaf carbon to  
485 nitrogen ratio (*leafcn\_picea*) and the specific leaf area at canopy top (*slatop\_picea*). GPP  
486 sensitivity for the moss PFT is dominated by the same three parameters, but for the moss  
487 PFT instead of *Picea* (*flnr\_moss*, *leafcn\_moss*, and *slatop\_moss*). For NPP, QVEGT and  
488 NEE, the highest sensitivity the maintenance respiration base rate *br\_mr*, similar to  
489 earlier results in Griffiths et al. (2017). The maintenance respiration temperature  
490 sensitivity  $Q_{10\_mr}$  is also a key parameter for NPP and NEE. The critical onset growing  
491 degree day threshold (*crit\_onset\_gdd*), which drives deciduous phenology in the spring  
492 for the *Larix* and shrub PFTs, is an important parameter for NPP and NEE. *flnr\_picea* is  
493 important for both NPP and QVEGT. For NPP\_moss and QVEG\_moss, *leafcn\_moss* is  
494 and the ratio of non-photosynthesizing tissue to photosynthesizing tissue (*npt\_moss*) are  
495 sensitive. For TOTVEGC and NEE, vegetation mortality (*r\_mort*) is also a sensitive  
496 parameter. For the site-level quantities of interest, at least 10 parameters contribute  
497 significantly to the uncertainty, illustrating the complexity of the model and large number  
498 of processes contributing to uncertainty in SPRUCE predictions. For the moss variables,

499 there are some cases where significant sensitivities exist for non-moss PFT parameters.  
 500 For example, *leafcn\_shrub* is the seventh most sensitive parameter for GPP\_moss,  
 501 indicating that competition between the PFTs for resources may be important. In this  
 502 case, uncertainty about parameters on one PFT may drive uncertainties in the simulated  
 503 productivity of other PFTs.



504

505 Figure 2 Sensitivity analysis of ELM-SPRUCE for selected parameters (Table 2 and 3). The  
 506 Colored bars indicate the fraction of variance in site gross primary productivity (GPP), moss-only  
 507 NPP (GPP\_MOSS), site net primary productivity (NPP), moss-only NPP (NPP\_MOSS), total  
 508 vegetation transpiration (QVEGT), moss evaporation (QVEG\_MOSS), site net ecosystem  
 509 exchange (NEE) and total vegetation carbon (TOTVEGC) controlled by each parameter. The  
 510 legend shows the top 25 most influential parameters; the remaining parameters not shown have  
 511 sensitivities of no more than 0.01 for any of the outputs. All variables represent 2011-2017

512 average values over the ambient conditions. For parameters that are treated as PFT-dependent,  
513 the PFT is indicated with a suffix (picea, larix, shrub or moss)  
514

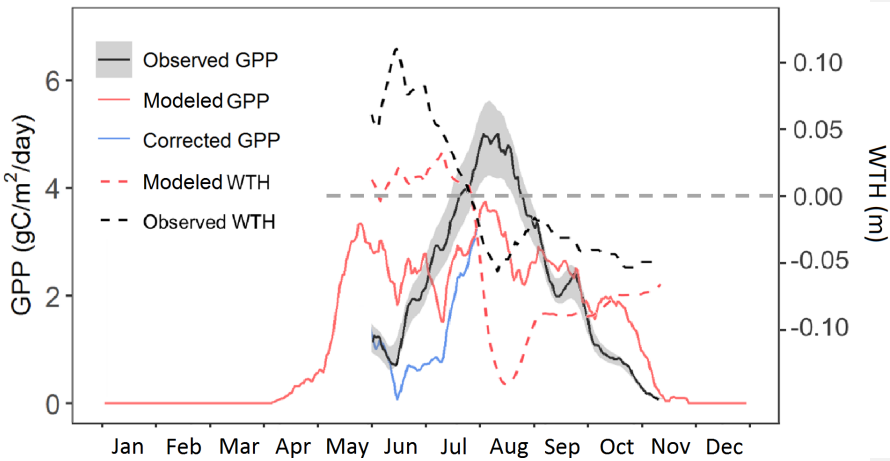
## 515 **4.2 Model evaluation**

516 Our model simulates GPP for vascular plants and *Sphagnum* moss in both  
517 hummock and hollow settings, with separate calculations for each PFT. Here we use the  
518 model estimate of GPP prior to downregulation by nutrient limitation from the ambient  
519 case, based on recent studies indicating that nutrient limitation effects are occurring  
520 downstream of GPP (Raczka et al. 2016; Metcalfe et al., 2017; Duarte et al. 2017). This  
521 treatment of nutrient limitation on GPP has been modified in a more recent version of  
522 ELM, and our moss modifications will be merged to that version as a next step. For now,  
523 by referring to the pre-downregulation GPP we are capturing the most significant impact  
524 of those changes for the purpose of comparison to observations.

525 Our model simulated two seasonal maxima of *Sphagnum* moss GPP, one at the  
526 end of May, and the other in August (Figure 3). Both peaks are lower than the maximum  
527 of observed (flux-partitioned) GPP, which occurs in August. Based on results of the  
528 sensitivity analysis, it could be that the base rate for maintenance respiration for moss is  
529 too high, causing an underestimate of NPP and biomass, which leads to a low bias in  
530 peak GPP.

531 During June and October, observations suggest that ELM\_SPRUCE over-predicts  
532 GPP. The model does limit GPP as a function of the depth of standing water on the bog  
533 surface (Eq. 7). The water table height (WTH) above the bog surface is being predicted  
534 by the model (dashed red line in Fig. 3), and while the seasonal pattern of higher water

535 table in the spring and lower water table in the fall agrees well with observations (dashed  
 536 black line in Fig. 3), the predicted WTH is generally too low by 5-10 cm. The modeled  
 537 WTH here is for hollow. We turned off the lateral transport when there is ice on the soil  
 538 layers above the water table to avoid an unreasonable amount of ice accumulation on the  
 539 frozen layers, which results in there is no flow from hummock to hollow. Forcing the  
 540 modeled GPP to respond to observed WTH (during the period with observations) gives a  
 541 pattern of increasing GPP through June and July which is more consistent with  
 542 observations (blue line in Fig. 3). We do not have observations for GPP earlier than June,  
 543 due to limitations of the instrumentation when the bog surface is flooded.



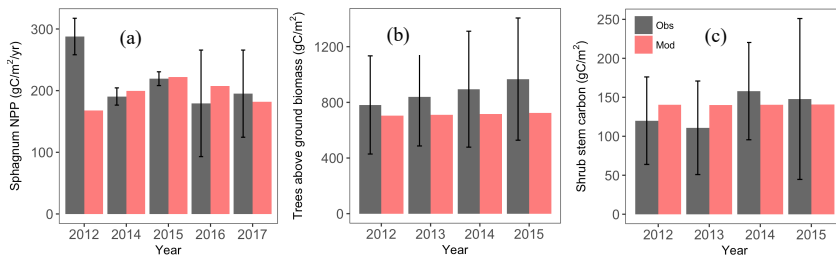
544  
 545  
 546 Figure 3. Predicted GPP (red solid line) compared with flux-partitioned GPP (black solid line,  
 547 GPP data was not used in the parameters optimization) of *Sphagnum* mosses for the year 2014.  
 548 The blue line is the predicted GPP corrected with the observed water table height. The dashed  
 549 black and red lines are observed and modeled water table height (the dashed gray line is the  
 550 hollow surface).  
 551  
 552

553 The model simulated reasonable annual values for *Sphagnum* NPP for the period  
 554 2014-2017 but showed much lower NPP compared with observation (139 vs. 288 g



555 C/m<sup>2</sup>/yr) for the year 2012 (Fig. 4a). Measurement uncertainties are larger in 2016-2017  
 556 than in earlier years, perhaps related to a new measurement protocol for those years, and  
 557 the model estimates are within measurement uncertainty bounds for years 2014-2017  
 558 (Griffiths et al., 2018; Norby et al., 2019). The observed *Sphagnum* NPP was measured at  
 559 different plots and each plot included different species abundances. As a result, the scaled  
 560 NPP includes spatial variations and uncertainty in species distribution (Norby and Childs,  
 561 2017).

562 Simulated tree above ground biomass is within the observed inter-plot variability  
 563 (Fig. 4b). Observations suggest an increasing trend in tree biomass, which was not  
 564 predicted by the model. The optimized parameters show increased mortality and  
 565 autotrophic respiration rate parameters compared to the default model (Table 3), which  
 566 causes the simulations to approach steady state relatively quickly after the 1974  
 567 disturbance. However, the sensitivity analysis also identifies these mortality and  
 568 maintenance respiration parameters as highly sensitive, therefore this simulated response  
 569 is uncertain. For the shrub stem carbon, the simulated mean from year 2012 to 2015 was  
 570 140.4 g C/m<sup>2</sup>, slightly higher than the observation (133.9 g C/m<sup>2</sup>) but well within the  
 571 observed range of inter-plot variability (Fig. 4c).



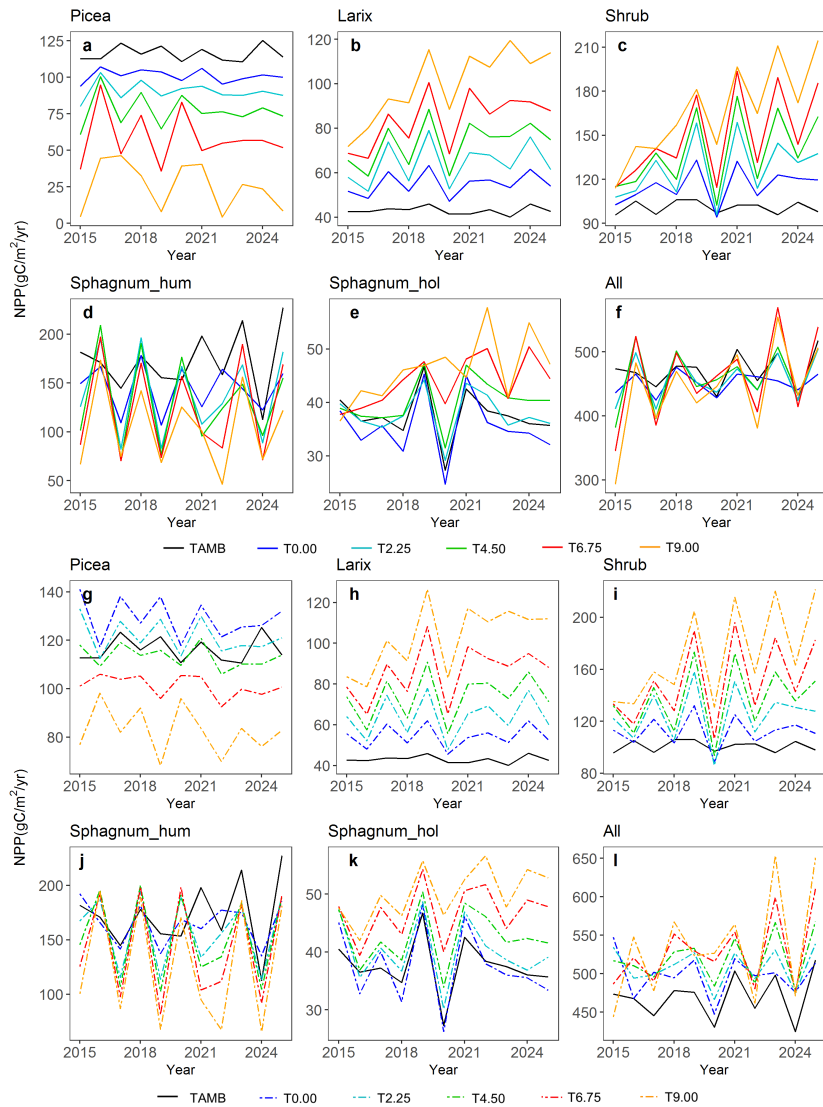
572

573 Figure 4. Predicted (red bars) *Sphagnum* NPP (left), aboveground tree biomass (middle) and  
574 shrub stem carbon (right) compared with the observations (black bars). Observed NPP data are  
575 based on growth of 12-17 bundles of 10 *Sphagnum* stems in 2012-2015 (unpublished data) and  
576 in two ambient plots by the method described by Norby et al. (2019) in 2016-2017 (data in  
577 Norby et al. 2017). [The \*Sphagnum\* NPP data of year 2015-2017, and aboveground tree biomass  
578 and shrub stem carbon of year 2014-2015 are independent of the related parameters  
579 optimization.](#)

### 581 4.3 Simulated carbon cycle response to warming and elevated atmospheric CO<sub>2</sub> 582 concentration

583 Different PFTs demonstrated different warming responses for both ambient CO<sub>2</sub>  
584 and elevated CO<sub>2</sub> concentration conditions (Fig. 5). Both *Larix* and shrub NPP increased  
585 with warming under both CO<sub>2</sub> concentration conditions (Fig. 5 b, c, h and i). In addition,  
586 CO<sub>2</sub> fertilization stimulates the growth of these two PFTs and the fertilization effect  
587 further increases with warming (Fig. S1, GPP increases more under elevated CO<sub>2</sub>  
588 condition than the ambient case). In contrast, *Picea* NPP decreased with warming levels  
589 (Fig. 5 a and g) for both CO<sub>2</sub> conditions. For *Sphagnum*, NPP decreased in hummocks  
590 but increased in hollows with increasing temperature (Fig. 5 d, e, j and k). [The CO<sub>2</sub>  
591 fertilization also stimulate the grow of the \*Picea\* and \*Sphagnum\* PFTs \(Fig. 5 a, d, e g, j  
592 and k\).](#) The enclosure-total NPP for all PFTs responded differently to the warming only  
593 and warming with elevated CO<sub>2</sub> (Fig. 5 f and l). The enclosure-total NPP for each  
594 warming level changed less under the ambient CO<sub>2</sub> condition than those with elevated  
595 CO<sub>2</sub> condition, and NPP decreased with warming in most of years under ambient CO<sub>2</sub>  
596 condition but increased under elevated CO<sub>2</sub> condition (Fig.5 f and l). This result  
597 demonstrated that the elevated CO<sub>2</sub> scenario changes the sign of the NPP warming  
598 response for the bog peatland ecosystem.

Formatted: Font: Italic



599  
600  
601  
602  
603  
604

Figure 5 predicted NPP response to warming with ambient atmospheric CO<sub>2</sub> (a-f, solid lines) and warming with elevated atmospheric CO<sub>2</sub> concentration (g-l, dash lines), the black solid line TAMB is the ambient temperature and CO<sub>2</sub> case, T0.00 to T9.00 means increasing temperature from 0°C to 9°C

605 Compared with the ambient biomass, the biomass of black spruce (*Picea*)  
606 significantly decreased but the biomass of *Larix* significantly increased under the greatest  
607 warming treatment (+9.00°C, Fig.6). Biomass of shrub and hollow *Sphagnum* also  
608 increased, but less than did *Larix*. The hummock *Sphagnum* biomass also showed strong  
609 correlation with water table height at roughly a 3-month lag (the maximum correlation  
610 occurs with an 82-day lag,  $R^2=0.56$ ). NPP is allocated instantaneously into biomass. A  
611 positive NPP anomaly caused by water table shifts leads to higher LAI, which also  
612 increases future productivity for some amount of time even if the water table returns to  
613 normal. *Sphagnum* biomass has a 1-year turnover time in the simulation. This  
614 combination of effects leads to a roughly 3-month timelag. Due to the relative lower  
615 height of the water table in the hummock than the hollow, the simulated hummock  
616 *Sphagnum* were more significantly water-stressed than the hollow *Sphagnum* as the water  
617 table height declines. This is consistent with multiple studies finding an increase in  
618 temperatures associated with drought (low water table height) reducing *Sphagnum*  
619 growth (Bragazza et al., 2016; Granath et al., 2016; Mazziotta et al., 2018). We plotted  
620 the predicted canopy evaporation for hummock and hollow *Sphagnum* responses to  
621 warming and found that both hummock and hollow *Sphagnum* canopy evaporation  
622 increase with warming for both ambient and elevated atmospheric CO<sub>2</sub> conditions despite  
623 the *Larix* and shrubs are growing with warming. Moreover, the hollow *Sphagnum* canopy  
624 evaporation warming response is stronger than that of the hummock *Sphagnum* (Fig. S2).  
625 In summary, the growth of bog vegetation is predicted to have species-specific warming  
626 responses that differ in sign and magnitude.

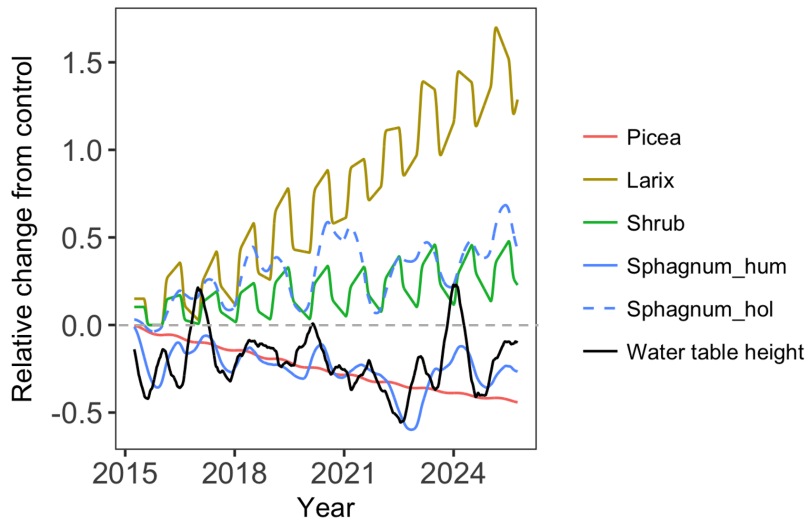
Formatted: Font: Italic

Formatted: Font: Italic

Formatted: Font: Italic

Formatted: Font: Italic

Formatted: Font: Italic



627  
628 Figure 6 The relative changes of biomass for different PFTs and water table height (the weighted  
629 average between hummock and hollow) between +9.00 °C treatment case and the ambient case  
630 (+9.00 °C / ambient - 1)

631 **5. Discussion**

632  
633 *Sphagnum* moss is the principal plant involved in the peat accumulation in peatland  
634 ecosystems, and effective characterization of its biophysical and physiological responses  
635 has implications for predicting peatland and global carbon, water and climate feedbacks.  
636 This study moves us closer to our long-term goal of improving the prediction of peatland  
637 water, carbon and nutrient cycles in ELM *SPRUCE*, by introducing a new *Sphagnum*  
638 moss PFT, implementing water content dynamics and photosynthetic processes for this  
639 nonvascular plant. The *Sphagnum* model development combined with our previous  
640 hummock-hollow microtopography representation and laterally-coupled two-column  
641 hydrology scheme enhance the capability of ELM\_ *SPRUCE* in simulating high-carbon  
642 wetland hydrology and carbon interactions and their responses to plausible environmental  
643 changes.

Formatted: Font: Italic

Deleted: and

645

## 646 5.1 Uncertainties in simulating *Sphagnum* productivity

647 Our predicted peak GPP is similar to the results found by Walker et al. (2017)  
648 when they calculated the internal resistance to CO<sub>2</sub> diffusion as a function of *Sphagnum*  
649 water content using a stand-alone photosynthesis model. In both cases, the predicted peak  
650 GPP is lower than observations. Walker et al. (2017) were, however, able to capture the  
651 observed peak magnitude with a combination of light extinction coefficient, canopy  
652 clumping coefficient, maximum shoot area index (SAI), and a logistic function  
653 describing the effective *Sphagnum* SAI in relation to water table. Here we used model  
654 default values for the light extinction and canopy clumping coefficients. While the water  
655 table impacts *Sphagnum* productivity in our simulation, modeled leaf (or shoot) area  
656 index (LAI) is mainly controlled by NPP and turnover. In addition, we use the default  
657 formulation for acclimation of V<sub>cmax</sub> in ELM which is based on a 10-day mean growing  
658 temperature. At this point we don't have sufficient measurements to test this assumption,  
659 but we can prioritize these measurements in the future. *Sphagnum* temperature is  
660 computed from surface energy balance but because the current model doesn't have the  
661 capacity to estimate the shading effects from trees and shrubs, this may be overestimated.  
662 Moreover, biases in predicted water table height contribute to errors in the calculated  
663 submergence effect. Improving these biases and assuming an exponential rather than a  
664 linear CO<sub>2</sub> uptake profile may improve representation of the submergence effect. All  
665 these aspects may be attribute to the biases of the simulated *Sphagnum* GPP. We can  
666 consider this in the future when we have more detailed measurements. Further  
667 investigation is thus needed to understand how representative the chamber-based

Formatted: Space After: 0 pt, Widow/Orphan control, Adjust space between Latin and Asian text, Adjust space between Asian text and numbers, Tab stops: Not at 0.5"

Formatted: Font: Italic

Formatted: Subscript

Formatted: Font: Italic

668 observations from Walker et al. (2017) are of the larger-scale SPRUCE enclosures, and to  
669 reconcile these GPP estimates with plot-level NPP observations (Norby et al., 2019).

Formatted: Font color: Red

670 The hydrology cycle, especially water table depth (WTD) is also a key factor that  
671 influences the seasonality of GPP in *Sphagnum* mosses (Lafleur et al., 2005; Riutta 2007,

672 Sonnentag et al, 2010; Grant et al., 2012; Kuiper et al., 2014; Walker et al, 2017). One  
673 key feedback is if the water table declines, there can be enhanced decomposition and  
674 subsidence of the peat layer, which brings the surface down closer to the water table  
675 again. But we currently did not consider the peat layer elevation changes in our model  
676 and this will be one of the future development directions. The capillary rise plays into the

Formatted: Font: Italic

677 *Sphagnum* hydrological balance, which varies depending on water table depth and  
678 evaporative demand. At short timescales or under rapidly changing conditions, there may  
679 not be equilibration between the *Sphagnum* water content and the peat moisture.

Formatted: Font: Italic

680 Generally, the *sphagnum* water content will equilibrate with the peat on a daily basis  
681 outside the plot since the dew point is often reached at night. But inside the warmer plots  
682 since the vapor pressure deficit does not go to zero some disequilibrium could remain.

683 High-frequency latent heat flux data from the site are currently lacking, but could help to  
684 constrain these effects in the future. The current phenology observations also include if  
685 *Sphagnum* hummock and hollow are wet or dry, and we could look at the relationship

Formatted: Font: Italic

686 with soil water content sensors in the future. Moreover, the equilibration time between  
687 peat moisture and moss water content is reasonable fast, but the timescales for rewetting  
688 should change as the peat dries since the cross section for capillary rise will decline and  
689 thus the maximum flux to the surface will decline. So, at some point, between gravity  
690 potential and reduced hydraulic conductivity the capillarity will not satisfy evaporative

691 demand (Personal discussion with field expert Jeffrey Warren). Previous studies have  
692 reported that drier and warmer future climates can lower the water table, affecting the  
693 resilience of long-term boreal peatland carbon stocks (Limpens et al., 2008, Dise, 2009,  
694 Frolking et al., 2011). WTD drawdown affects the net ecosystem productivity of boreal  
695 peatlands through its effects on ecosystem respiration and GPP. The interactions between  
696 WTD and GPP, however, vary across peatlands and influence both vascular and  
697 nonvascular plant GPP in different ways (Lafleur et al., 2005). For instance, nonvascular  
698 plants mostly access water in the near surface shallow peat layers. These layers, however,  
699 can drain quickly with receding WTD and high nonvascular evaporative demand, and  
700 thus depend on water supply through capillary rise or precipitation (Dimitrov et al., 2011,  
701 Peichl et al., 2014, Druel et al., 2017). If recharge is not adequate, near-surface peat  
702 desiccation occurs thereby cutting off the supply of water to *Sphagnum*, which  
703 subsequently dries, leading to rapid decline in GPP (Lafleur et al., 2005, Riutta 2008,  
704 Sonnentag et al., 2010, Sulman et al., 2010, Dimitrov et al., 2011, Kuiper et al., 2014,  
705 Peichl et al., 2014). Thus, for the *Sphagnum* mosses desiccation occurs and the time  
706 needed before recovery to optimum photosynthetic capacity should be taken into account  
707 in our future work. Alternately, under saturated conditions when the water table is close  
708 to the *Sphagnum* surface, *Sphagnum* photosynthesizing tissue can become submerged or  
709 surrounded by a film of water that is likely to reduce the effective LAI of the *Sphagnum*  
710 and thus reduce photosynthesis (Walker et al., 2017). Submerged *Sphagnum* can take up  
711 carbon derived from CH<sub>4</sub> via symbiotic methanotrophs (Raghoebarsing et al., 2005), but  
712 in any cases CO<sub>2</sub> diffusion for photosynthesis will dramatically decrease under water.  
713 Larmola et al. (2014) also reported that the activity of oxidizing bacteria provides not

Deleted:

Formatted: Font: 12 pt, Font color: Auto

Deleted: For instance, nonvascular plants mostly access water in the near surface shallow peat layers.

Formatted: Font: Not Italic

Formatted: Font: 12 pt, Font color: Auto

Formatted: Font: 12 pt



717 only carbon but also nitrogen to peat mosses and, thus, contributes to carbon and nitrogen  
718 accumulation in peatlands, which store approximately one-third of the global soil carbon  
719 pool. We currently didn't consider this kind of CH<sub>4</sub> associated carbon and nitrogen  
720 uptake by *Sphagnum*.  
721 The live green *Sphagnum* moss layer buffers the exchange of energy and water at  
722 soil surface and regulates the soil temperature and moisture because of its high-water  
723 holding capacity and the insulating effect (McFadden et al., 2003; Block et al., 2011;  
724 Turesky et al, 2012; Park et al., 2018). Currently, we apply the same method for the  
725 hummock and hollow *Sphagnum* water content prediction and can test the model against  
726 the measured data when more data are available. Our model still can predict *Sphagnum*  
727 water content differences between these microtopographies as expected, with the water  
728 content of hollows greater than that of hummocks though. In addition, our model is able  
729 to represent the self-cooling effect, although we do not yet have measurements available  
730 to validate the model. The relationship of the differences between vegetation temperature  
731 (TV) and 2m air temperature (TBOT) (TV-TBOT) and canopy evaporation for both  
732 hummock and hollow *Sphagnum* demonstrated that the differences of TV-TBOT was  
733 negative and the canopy evaporation had a negative relationship with TV-TBOT (Fig.  
734 S3). Moreover, Walker et al., (2017) reported that the function of *Sphagnum* water  
735 content to soil water content or to water table depth they used for the SPRUCE site was  
736 empirical and may not be representative for peatland ecosystem. To better represent the  
737 peatland ecosystem in our model, we will eventually treat the *Sphagnum* mosses as the  
738 "top" soil layer with a lower thermal conductivity and higher hydraulic capacity  
739 (Beringer et al., 2001; Wu et al., 2016; Porada et al., 2016).

Formatted: Font: 12 pt

Formatted: Font: 12 pt, Subscript

Formatted: Font: 12 pt

Formatted: Font color: Red

Formatted: Normal

Formatted: Font: Italic

Formatted: Font: Times New Roman

Formatted: Font: Italic

Formatted: Font: Italic

Formatted: Font: Italic

Formatted: Font: Italic

Formatted: Font color: Red

740

## 741 5.2 Predicted warming and elevated CO<sub>2</sub> concentration response uncertainties

742

743

744

745

746

747

748

749

750

751

752

753

754

755

756

757

758

759

760

761

762

Our model warming simulations suggested that increasing temperature reduced the *Picea* growth but increased the growth of *Larix* under both ambient and elevated atmospheric CO<sub>2</sub> conditions. The main reason for this model difference in response for the two tree species is that despite their similar productivity under ambient conditions, *Picea* has more respiring leaf and fine root biomass because of lower specific leaf area, longer leaf longevity, and higher fine root allocation. Therefore, warming results in a much larger increase in maintenance respiration relative to changes in NPP for *Picea* compared to *Larix* (Fig. 5 and Fig. S4). Increased tree growth and productivity in response to the recent climate warming for high-latitude forests has been reported (Myneni et al., 1997, Chen et al. 1999, Wilming et al. 2004, Chavardes, 2013). On the other hand, reductions in tree growth and negative correlations between growth and temperature also have been shown (Barber et al., 2000; Wilmking et al., 2004; Silva et al., 2010; Juday and Alix 2012; Girardin et al., 2016; Wolken et at., 2016).

Our model also predicted increasing growth of shrubs with increased temperature, similar to simulated increase in shrub cover caused mainly by warmer temperatures and longer growing seasons reported by Miller and Smith (2012) using their model LPJ-GUESS. In addition, several other modelling studies have also found increased biomass production and LAI related to shrub invasion and replacement of low shrubs by taller shrubs and trees in response to increased temperatures in tundra regions (Zhang et al., 2013; Miller and Smith, 2012; Wolf et al., 2008; [Porada et al., 2016](#); Rydssa et al., 2017).

**Deleted:** Alternately, under saturated conditions when the water table is close to the *Sphagnum* surface, *Sphagnum* photosynthesizing tissue can become submerged or surrounded by a film of water that is likely to reduce the effective LAI of the *Sphagnum* and thus reduce photosynthesis (Walker et al., 2017). One study reported that submerged *Sphagnum* can take up carbon derived from CH<sub>4</sub> via symbiotic methanotrophs (Raghoebarsing et al., 2005), but in any cases CO<sub>2</sub> diffusion for photosynthesis will dramatically decrease under water.

**Formatted:** Space After: 0 pt, Widow/Orphan control, Adjust space between Latin and Asian text, Adjust space between Asian text and numbers, Tab stops: Not at 0.5"

**Formatted:** Subscript

**Deleted:** 2

774 The responses of *Sphagnum* mosses to warming simulated by ELM\_SPRUCE  
775 showed that *Sphagnum* growth in hollows was consistently higher with increased  
776 temperatures, where water availability was not limiting. *Sphagnum* growing on  
777 hummocks, on the other hand, showed negative warming responses that are related to the  
778 strong dependency on water table height. A Recent study of the same SPRUCE site  
779 (Norby et al. 2019) had suggested that the hummock-hollow microtopography had a  
780 larger influence on *Sphagnum* responses to warming than species-specific traits. In  
781 addition, the previous studies had demonstrated that the most dominant mechanism of  
782 *Sphagnum* warming response was probably through the effect of warming on depth to the  
783 water table and water content of the acrotelm, both of them responded to increasing  
784 temperature (Grosvernier et al., 1997; Rydin, 1985; Weltzin et al., 2001; Norby et al.,  
785 2019). Moreover, desiccation of capitula due to increased evaporation associated with  
786 higher temperatures and vapor pressure deficits can reduce *Sphagnum* growth  
787 independent of the water table depth (Gunnarsson et al., 2004). We currently used the  
788 same parameters for both hummock and hollow, but could consider species differences in  
789 the future. Norby et al. (2019) investigated different *Sphagnum* species at the same site  
790 and reported there was no support for the hypothesis that species more adapted to dry  
791 conditions (e.g., *S. magellanicum* and *Polytrichum* mainly on hummocks) would be more  
792 resistant to the stress and would increase in dominance, and both hummock and hollow  
793 *sphagnum* are declining with warming despite the differences between them. This  
794 declining trend may be in part due to increased shading from the shrub layer, which is  
795 expanding with warming.

Deleted: and

Formatted: Font: Italic

Formatted: Font: Not Italic

Formatted: Font: Italic

797 Ecosystem warming can have direct and indirect effects on *Sphagnum* moss  
798 growth. The growth of *Sphagnum* may be reduced directly by higher air temperature, due  
799 to the relatively low temperature optima of moss photosynthesis (Hobbie et al., 1999; Van  
800 Gaalen, 2007; Walker et al., 2017). On the other hand, increased shading by the shrub  
801 canopy and associated leaf litter could indirectly decrease moss growth (Chapin et al.,  
802 1995; Hobbie and Chapin 1998; Van der Wal et al., 2005; Walker et al., 2006; Breeuwer  
803 et al., 2008). In contrast, other studies suggest that *Sphagnum* growth can be promoted  
804 via a cooling effect of shading on the peat surface, by alleviating photo-inhibition of  
805 photosynthesis and also by reducing evaporation stress (Busby et al., 1978; Murray et al.,  
806 1993; Man et al., 2008; Walker et al., 2015; Bragazza et al., 2016; Mazziotta et al., 2018).  
807 Our model sensitivity analysis also indicated that the parameters of Shrub showing  
808 significant sensitivities to *Sphagnum* mosses GPP, indicating that competition between  
809 the PFTs for resources might be important. Moreover, ELM\_SPRUCE did predict  
810 enhancement of shrub and *Larix* tree with increased temperatures with both ambient and  
811 elevated CO<sub>2</sub> conditions (the leaf area increasing with warming, Fig. S3). Currently  
812 ELM\_SPRUCE does not include light competition among multiple PFTs, and thus does  
813 not represent cross-PFT shading effects, which may contribute to the warming and  
814 elevated CO<sub>2</sub> response differences between our model prediction and observed result of  
815 Norby et al. (2019). Meanwhile, we have fixed cover fraction for PFTs in our model may  
816 also contribute to the disagreement of predicted and observed warming responses. While  
817 Norby et al. (2019) showed that the fractional cover of different *Sphagnum* species  
818 declined with warming.

Formatted: Font: Italic

Deleted: Previous studies have shown that moss growth

Deleted: , and can be reduced by water stress (Norby et al., 2019)

Deleted: Moreove

Deleted: r

Deleted: O

Formatted: Font: Italic

Moved (insertion) [1]

Deleted: oes

Deleted:

Deleted: .

Formatted: Font: Italic

828 *Sphagnum* mosses are sitting on top of high CO<sub>2</sub> sources. CH<sub>4</sub> can be a significant  
 829 carbon sources of submerged *Sphagnum* (Raghoebarsing et al., 2005; Larmola et al,  
 830 2014); refixation of CO<sub>2</sub> derived from decomposition processes also is an important  
 831 source of carbon for *Sphagnum* (Rydin and Clymo, 1989; Turetsky and Wieder, 1999).  
 832 The effects of the elevation of atmospheric CO<sub>2</sub> on *Sphagnum* moss are currently  
 833 disputed, with studies indicating an increase in growth rate (Jauhiainen and Silvde 1999;  
 834 Heijmans et al. 2001a; Saarnio et al. 2003), decreases in growth rate (Grosvernier et al.  
 835 2001; Fenner et al. 2007) and no response (Van der Heijden et al. 2000; Hoosbeek et al.  
 836 2002; Toet et al. 2006). Norby et al. (2019) indicated that no growth stimulation of both  
 837 hummock and hollow *Sphagnum* under elevated CO<sub>2</sub> condition, but significant negative  
 838 effects of elevated CO<sub>2</sub> on *Sphagnum* NPP in year 2018 at the same study site.  
 839 Contrasting responses between *Sphagnum* species are thought to be coupled with the  
 840 water availability. In contrast, our model results showed that both hummock and hollow  
 841 *Sphagnum* growths were stimulated by the elevated CO<sub>2</sub> concentration, which may be  
 842 attributed to the fact that we did not consider the light competition between the PFTS  
 843 (shrub and tree shading effects) and use a fixed cover fraction of *Sphagnum*.  
 844 The CO<sub>2</sub> vertical concentration profile is assumed to be uniform in the  
 845 simulations. In the experiment, the enclosure's regulated additions of pure CO<sub>2</sub> are  
 846 distributed to a manifold that splits the gas into four equal streams feeding each of the  
 847 four air handling units (Hanson et al., 2017 Fig. 2a), and is injected into the ductwork of  
 848 each furnace just ahead of each blower and heat exchanger. Horizontal and vertical  
 849 mixing within each enclosure homogenizes the air volume distributing the CO<sub>2</sub> along  
 850 with the heated air. The horizontal blowers in the enclosures together with external wind

- Formatted: Font: Italic
- Formatted: Subscript
- Formatted: Subscript
- Formatted: Font: Italic
- Formatted: Subscript
- Formatted: Font: Italic
- Formatted: Subscript
- Formatted: Font: Italic
- Formatted: Subscript
- Formatted: Font: Italic
- Formatted: Subscript
- Formatted: Font: Italic
- Formatted: Subscript
- Formatted: Font: Italic
- Formatted: Font: Font color: Blue
- Formatted: Tab stops: Not at 0.5" + 2.69"

851 eddies ensure vertical mixing. We do not have routine automated CO<sub>2</sub> concentration data  
852 below 0.5m. The moss layer may well be experiencing higher concentrations than  
853 assumed by the model, but such an impact will be minimized during daylight hours.  
854 Preliminary isotopic measurements imply a significant fraction of carbon assimilated by  
855 the moss may come from subsurface respired CO<sub>2</sub> (i.e., CO<sub>2</sub> with older <sup>14</sup>C signatures  
856 predating bomb carbon that can only be sourced from deeper peat, Hanson et al., 2017).  
857 However, the observed elevated CO<sub>2</sub> response is smaller than simulated (Hanson et al.,  
858 2020). Understanding the drivers of elevated CO<sub>2</sub> response or lack thereof is a key topic  
859 for future work and we will consider this effect in future assessments of the isotopic  
860 carbon budgets for the SPRUCE study.  
861 To better investigate the *Sphagnum* warming and elevated CO<sub>2</sub> responses, we should  
862 also focus on revealing the interactions with Shrub and nitrogen availability (Norby et al.,  
863 2019). Nitrogen (N<sub>2</sub>) fixation is a major source of available N in ecosystems that receive  
864 low amounts of atmospheric N deposition, like boreal forests and subarctic tundra (Lindo  
865 et al., 2013, Weston et al, 2015, Rousk et al., 2016, Kostka et al., 2016). For example,  
866 diazotrophs are estimated to supply 40-60% of N input to peatlands (Vile et al., 2014)  
867 with high accumulation of fixed N into plant biomass (Berg et al., 2013). Nevertheless,  
868 N<sub>2</sub> fixation is an energy costly process and is inhibited when N availability and reactive  
869 nitrogen deposition is high (Gundale et al., 2011; Ackermann et al., 2012; Rousk et al.,  
870 2013). This could limit ecosystem N input via the N<sub>2</sub> fixation pathway. We are measuring  
871 *Sphagnum* associated N<sub>2</sub> fixation at the SPRUCE site and found that rates decline with  
872 increasing temperature (Carrell et al. 2019 Global Change Biology). We are continuing  
873 these measurements to see if they correlate with the GPP empirical relationship from

Formatted: Subscript

Formatted: Superscript

Formatted: Subscript

Formatted: Subscript

Formatted: Font color: Red

**Moved up [1]:** ELM\_SPRUCE does predict enhancement of shrub and Larix tree with increased temperatures with both ambient and elevated CO<sub>2</sub> conditions (the leaf area increasing with warming, Fig. S3). Norby et al. (2019) showed that the fractional cover of different Sphagnum species declined with warming, but while ELM\_SPRUCE allows the canopy density of PFTs to change prognostically,

**Deleted:** ELM\_SPRUCE does predict enhancement of of shrub and Larix tree with increased temperatures with both ambient and elevated CO<sub>2</sub> conditions (the leaf area increasing with warming, Fig. S3). Norby et al. (2019) showed that the fractional cover of different Sphagnum species declined with warming, but while ELM\_SPRUCE allows the canopy density of PFTs to change prognostically, their fractional cover is held constant.

Formatted: Font: Italic

Formatted: Subscript

890 Cleveland (1999), or if temperature disrupts that association. Once finished, results will be  
891 used to represent N fixation by the Sphagnum layer and testing with measurements.

Formatted: Font: Times New Roman

892 It is also encouraging that while we did not use leaf-level gas exchange  
893 observations in our optimization, the increased maintenance respiration base rate and  
894 temperature sensitivity compared to default (table 2) is largely consistent with pre-  
895 treatment leaf level observations (Jensen et al., 2019). In the future, a multi-scale  
896 optimization framework that can assimilate leaf and plot-level observations  
897 simultaneously should lead to improved model predictions and reduced uncertainties for  
898 the treatment simulations. If similar patterns observed in ambient conditions continue  
899 during the treatments, incorporating seasonal variations in leaf photosynthetic parameters  
900 may also further improve the simulated response to warming (Jensen et al., 2019).

901 Overall, while the sensitivity analysis is useful to indicate the key parameters and  
902 mechanisms responsible for uncertainty, our ability to quantify prediction uncertainty is  
903 limited because we consider only a single simulation with optimized parameters. Ideally,  
904 we should perform a model ensemble that represents the full range of posterior  
905 uncertainty over simulations that are consistent with the pre-treatment observations, and  
906 also a range of possible future meteorological conditions. This is currently being done for  
907 SPRUCE with the TECO carbon cycle model (Jiang et al., 2018), but the computational  
908 expense of ELM\_SPRUCE currently prohibits this approach. By combining new  
909 surrogate modeling approaches (e.g. Lu et al., 2019) with MCMC techniques, it may be  
910 possible to achieve this in the near future. This will help to reduce prediction  
911 uncertainties, which currently prevail in the future carbon budget of peatlands and its  
912 feedback to climate change (McGuire et al., 2009).

913 The algorithms used to represent moss (e.g. Williams and Flanagan) are  
914 transferable to and have been applied by other modeling groups in other  
915 peatlands. However, we expect that certain parameters will vary, for example, the  
916 microtopographic parameters, the relationship between peat moisture and internal water  
917 content, and moss properties such as C:N ratio. The parameter sensitivity analysis  
918 informs us as to the most important parameters responsible for prediction uncertainty,  
919 and can inform how to prioritize these measurements. Collecting these measurements  
920 from a variety of sites will be a necessary preliminary exercise. In addition to the  
921 simulations aimed at improved understanding of bog response to experimental  
922 manipulations at the plot-scale, we are pursuing model implementations at larger spatial  
923 scales. The model framework described in this study is capable of performing regional  
924 simulations, although the current simulations were designed for mechanistic  
925 understanding of *Sphagnum* mosses hydrological and physiological dynamics at the plot-  
926 level.

## 928 **6. Summary**

929 In this study, we reported the development of a *Sphagnum* moss PFT and  
930 associated processes within the ELM\_SPRUCE model. Before being used to examine the  
931 ecosystem response to warming and elevated CO<sub>2</sub> at a temperate bog ecosystem, the  
932 updated model was evaluated against the observed *Sphagnum* GPP and annual NPP,  
933 aboveground tree biomass and shrub stem biomass. The new model can capture the  
934 seasonal dynamics of moss *Sphagnum* GPP, but with lower peak GPP compared to site-  
935 level observations, and can predict reasonable annual values for *Sphagnum* NPP but with

Formatted: Font: 12 pt

Deleted: ¶

### 5.3 Outstanding issues and future directions¶

→ The present modeling framework works well for hydrological dynamics (Shi et al., 2015), vegetation responses (this study), and reconstructing CH<sub>4</sub> dynamics (Ricciuto et al., in review) within the S1-Bog in Minnesota. It will thus be migrated into the E3SM. However, more developments of ELM\_SPRUCE are still needed before widespread applications.¶

The live green moss layer buffers the exchange of energy and water at soil surface and regulates the soil temperature and moisture because of its high-water holding capacity and the insulating effect (McFadden et al., 2003; Block et al., 2011; Turesky et al., 2012; Park et al., 2018). Nevertheless, we currently include only one *Sphagnum* moss PFT, and will eventually treat the *Sphagnum* mosses as the “top” soil layer with a lower thermal conductivity and higher hydraulic capacity than a mineral soil layer (Wu et al., 2016). We also intend to model light competition, the shading effect of shrub expansion, and the changes of *Sphagnum* community composition. Moreover, the new implementation would allow for the simulation of the moss layer acting as a barrier for the water and energy exchange from the underlying organic soil layer with the atmosphere. In addition, we also plan to investigate the ecosystem consequences of loss of *Sphagnum* from this ecosystem.¶

→ The current model version is not able to simulate the biogeophysical changes that occur due to the long-term accumulation of peat in the bog; however, previous literature reported that there is a need to develop relatively realistic peatland growth models where the rates of ecosystem processes are a function of climate and the inherent autogenic properties of peatlands (Frolking et al., 2010; Belyea and Baird, 2006; Dies, 2009). Thus, future work requires modeling the peat accumulation and associated feedbacks among hydrology, vegetation communities, and peat properties. This would also facilitate the simulation of basic patterns of peat accumulation over millennia in northern peatlands, including accumulation rates, vegetation and fen-bog transitions, and future impacts from the potential loss of peat under warming scenarios.¶

→ Nitrogen (N<sub>2</sub>) fixation is a major source of available N in ecosystems that receive low amounts of atmospheric N deposition, like boreal forests and subarctic tundra (Lindo et al., 2013; Weston et al., 2015; Rousk et al., 2016; Kostka et al., 2016). For example, diazotrophs are estimated to supply 40-60% of N input to peatlands (Vile et al., 2014) with high accumulation of fixed N into plant biomass (Berg et al., 2013). Nevertheless, N<sub>2</sub> fixation is an energy costly process and is inhibited when N availability and reactive nitrogen deposition is high (Gundale et al., 2011; Ackermann et al., 2012; Rousk et al., 2013). This could limit ecosystem N input via the N<sub>2</sub> fixation pathway. A recent study showed that N<sub>2</sub> fixation activity in the S1-bog was negatively correlated with temperature (Carrell et al., 2019). However, for the current ELM\_SPRUCE, N<sub>2</sub> fixation process is only tied to the whole-ecosystem NPP for all PFTs and is not mechanistic. We will focus on this process in future model development.¶

In addition to the simulations aimed at improved understanding of bog response to experimental

... [1]



1070 lower interannual variation. Our model largely agrees with observed tree and shrub  
1071 biomass. The model predicts that different PFTs responded differently to warming levels  
1072 under both ambient and elevated CO<sub>2</sub> concentration conditions. The NPP of the two  
1073 dominant tree PFTs (black spruce and *Larix*) showed contrasting responses to warming  
1074 scenarios (increasing with warming for *Larix* but decreasing for black spruce), while  
1075 shrub NPP had similar warming response to *Larix*. Hummock and hollow *Sphagnum*  
1076 showed opposite warming responses: hollow *Sphagnum* shows generally higher growth  
1077 with warming, but the hummock *Sphagnum* demonstrates more variability and strong  
1078 dependence with water table height. The ELM predictions further suggest that the effects  
1079 of CO<sub>2</sub> fertilization can change the direction of the warming response for the bog  
1080 peatland ecosystem, though observations of *Sphagnum* species at the site does not yet  
1081 appear to support this (Norby et al. 2019).

1082 Data availability. The model code we used is available here:  
1083 [https://github.com/dmricciuto/CLM\\_SPRUCE](https://github.com/dmricciuto/CLM_SPRUCE). The datasets and scripts were used for the figures  
1084 is here: [https://github.com/dmricciuto/CLM\\_SPRUCE/tree/master/analysis/Shietal2020](https://github.com/dmricciuto/CLM_SPRUCE/tree/master/analysis/Shietal2020)  
1085  
1086

#### 1087 **Acknowledgements**

1088 Research was supported by the U. S. Department of Energy, Office of Science,  
1089 Biological and Environmental Research Program. Oak Ridge National Laboratory is  
1090 managed by UT-Battelle, LLC, for the US Department of Energy under contract DE-  
1091 AC05-00OR22725.

1092

#### 1093 **References:**

Deleted:

1095 Ackermann, K., Zackrisson, O., Rousk, J., Jones, D. L., and DeLuca, T. H.: N<sub>2</sub> fixation  
1096 in feather mosses is a sensitive indicator of N deposition in boreal forests, *Ecosystems*,  
1097 15, 986-998, 2012.

1098 Barber, V. A., Juday, G. P., and Finney, B. P.: Reduced growth of Alaskan white spruce  
1099 in the twentieth century from temperature-induced drought stress, *Nature*, 405,668-  
1100 673, 2000.

1101 ~~Beringer, J., Lynch, A., Chapin, F., Mack, M., and Bonan, G.: The Representation of~~  
1102 ~~Arctic Soils in the Land Surface Model: The Importance of Mosses, *J. Climate*, 14, 3324-~~  
1103 ~~3335, doi:10.1175/1520-0442(2001)014<3324:TROASI>2.0.CO;2, 2001.~~

1104 Berg, A., Danielsson, A., and Sevansson, B.H.: Transfer of fixed-N from N<sub>2</sub>-fixing  
1105 cyanobacteria associated with moss sphagnum riparium results in enhanced growth of  
1106 the moss, plant and soil, 362, 271-278, <https://doi.org/10.1007/s11104-012-1278-4>,  
1107 2013.

1108 ~~Blok, D., Heijmans, M., Schaepman-Strub, G., Van Ruijven, J., Parmentier, F.,~~  
1109 ~~Maximov, T., and Berendse, F.: The cooling capacity of mosses: Controls on water~~  
1110 ~~and energy fluxes in a Siberian tundra site, *Ecosystems*, 14, 1055-1065, 2011.~~

1111 Bond-Lamberty, B., Peckham, S. D., Ahl, D. E., and Gower, S. T.: Fire as the dominant  
1112 driver of central Canadian boreal forest carbon balance, *Nature*, 450, 89-92, 2007.

1113 Bragazza, L., Buttler, A., Robroek, B. J., Albrecht, R., Zaccone, C., Jassey, V. E., and  
1114 Signarbieux, C.: Persistent high temperature and low precipitation reduce peat carbon  
1115 accumulation, *Global Change Biology*, 22, 4114-4123,  
1116 <https://doi.org/10.1111/gcb.13319>, 2016.

1117 Breeuwer, A., Heijmans, M. M., Robroek, B. J., and Berendse, F.: The effect of  
1118 temperature on growth and competition between *Sphagnum*  
1119 species, *Oecologia*, 156(1), 155-167, doi:10.1007/s00442-008-0963-8, 2008.

1120 Brown, S. M., Petrone, R. M., Mendoza, C., and Devito, K. J.: Surface vegetation  
1121 controls on evapotranspiration from a sub-humid Western Boreal Plain wetland,  
1122 *Hydrological Processes*, 24(8), 1072-1085, 2010.

1123 Busby, J.R., Bliss, L.C., and Hamilton, C.D.: Microclimate control of growth rates and  
1124 habitats of the Boreal Forest Mosses, *Tomenthypnum nitens* and *Hylocomium*  
1125 *splenden*, *Ecol Monogr*, 48, 95-110, 1978.

1126 Burrows, S.M., Maltrud, M.E., Yang, X., Zhu, Q., Jeffery, N., Shi, X., Ricciuto, D.M.,  
1127 Wang, S., Bisht, G., Tang, J., Wolfe, J. D., Harrop, B. E., Singh, B., Brent, L., Zhou,  
1128 Tian, Cameron-Smith P. J., Keen, N., Collier, N., Xu, M., Hunke, E.C., Elliott, S.M.,  
1129 Turner, A.K., Li, H., Wang, H., Golaz, J.-C., Bond-Lamberty, B., Hoffman, F.M.,  
1130 Riley, W.J., Thornton, P.E., Calvin, K., and Leung, L.R.: The DOE E3SM coupled  
1131 model v1.1 biogeochemistry configuration: overview and evaluation of coupled

Formatted: Font: Times New Roman, 12 pt

Formatted: Indent: Left: 0", First line: 0", Space  
Before: Auto, After: Auto

Formatted: Font: Times New Roman, 12 pt

Deleted: Belyea, L. R. and Baird, A. J.: Beyond "The  
limits to peat bog growth": Cross-scale feedback in peatland  
development, *Ecol. Monogr.*, 76, 299-322, 2006.

Deleted:

- 1136 carbon-climate experiments, *J. Adv. Model Earth Sy.*, **12**, e2019MS001766,  
 1137 <https://doi.org/10.1029/2019MS001766>, 2020,  
 1138 Gorham, E.: Northern peatlands: role in the carbon cycle and probable responses to  
 1139 climatic warming, *Ecological Applications*, **1**, 182-195, 1991.
- 1140 Camill, P. and Clark, J. S.: Long-term perspectives on lagged ecosystem responses to  
 1141 climate change: permafrost in boreal peatlands and the grassland/woodland boundary,  
 1142 *Ecosystems*, **3**, 534–544, 2000.
- 1143 [Chadburn, S., Burke, E., Essery, R., Boike, J., Langer, M., Heikenfeld, M., Cox, P., and](#)  
 1144 [Friedlingstein, P.: An improved representation of physical permafrost dynamics in](#)  
 1145 [the JULES land-surface model, \*Geosci. Model Dev.\*, \*\*8\*\*, 1493–1508, doi:10.5194/gmd-](#)  
 1146 [8-1493-2015, 2015.](#)
- 1147 Chapin, F. S. III, Shaver, G.R., Giblin, A.E., Nadelhoffer, K.J., and Laundre, J.A.:  
 1148 Responses of Arctic tundra to experimental and observed changes in climate, *Ecology*,  
 1149 **76**, 694-711, 1995.
- 1150 Carrell, A.A., Kolton, M., Warren, M.J., Kostka, J.E., and Weston, D. J.: Experimental  
 1151 warming alters the community composition, diversity, and N<sub>2</sub> fixation activity of peat  
 1152 moss (*Sphagnum fallax*) microbiomes, *Glob. Change Biol.*, **25**, 2993-3004,  
 1153 doi:10.1111/gcb.14715, 2019.
- 1154 Chavardes, R. D., L. D. Daniels, P. O. Waeber, J. L. Innes, and C. R. Nitschke.: Unstable  
 1155 climate-growth relations for white spruce in southwest Yukon, Canada, *Climatic*  
 1156 *Change*, **116**, 593-611, 2013.
- 1157 Chen, W. J., Black, T. A., Yang, P.C. Barr, A.G. Neumann, H. H., Nešić, Z., Blanken, P.  
 1158 D. Novak, M. D., Eley, J., Kettler, R., and Cuenca, R. H.: Effects of climatic variability  
 1159 on the annual carbon sequestration by a boreal aspen forest, *Glob. Change Biol.*, **5**, 41-  
 1160 53, 1999.
- 1161 Clymo, R. S. and Hayward, P.M.: The ecology of *Sphagnum*, in: *Bryophyte Ecology*,  
 1162 edited by: Smith, A. I. E., Chapman and Hall Ltd., London, New York, 229-289, 1982.
- 1163 Collatz, G.J., Ball, J.T., Grivet, C. and Berry, J.A.: Physiological and environmental-  
 1164 regulation of stomatal conductance, photosynthesis and transpiration - a model that  
 1165 includes a laminar boundary-layer, *Agricultural and Forest Meteorology*, **54**, 107-  
 1166 136, 1991.
- 1167 Collatz, G.J., Ribas-Carbo, M. and Berry, J.A.: Coupled photosynthesis- stomatal model  
 1168 for leaves of C<sub>4</sub> plants, *Australian Journal of Plant Physiology*, **19**, 519-538, 1992.
- 1169 Cornelissen, H.C., Lang, S.I., Soudzilovskaia, N.A., and During, H.J.: Comparative  
 1170 cryptogam ecology: a review of bryophyte and lichen traits that drive  
 1171 biogeochemistry, *Annals of Botany*, **99**, 987–1001, 2007.

Deleted: in review

Deleted: 19

Formatted: Font: Times New Roman, 12 pt

1174 Davidson, E. A. and Janssens, I. A.: Temperature sensitivity of soil carbon decomposition  
1175 and feedbacks to climate change, *Nature*, 440, 165-173, 2006.

1176 Dimitrov, D. D., Grant, R. F., LaFleur, P. M., and Humphreys, E.: Modelling the effects  
1177 of hydrology on gross primary productivity and net ecosystem productivity at Mer  
1178 Bleue bog, *J. Geophys. Res.-Biogeo*, 116, G04010, doi:10.1029/2010JG001586, 2011.

1179 Dorrepaal, E., Toet, S., van Logtestijn, R. S. P., Swart, E., van de Weg, M. J., Callaghan,  
1180 T. V., and Aerts, R.: Carbon respiration from subsurface peat accelerated by climate  
1181 warming in the sub- arctic, *Nature*, 460, 616-619, 2009.

1182 [Druel, A., Peylin, P., Krinner, G., Ciais, P., Viovy, N., Peregon, A., Barstrikov, V.,](#)  
1183 [Kosykh, N., Mironycheva-Tokareva, N., Towards a more detailed representation of](#)  
1184 [high-latitude vegetation in the global land surface model ORCHIDEE \(ORC-HL-](#)  
1185 [VEGv1.0\), \*Geoscientific Model Development\*, 10\(12\), 4693–4722,](#)  
1186 <https://doi.org/10.5194/gmd-10-4693-2017>, 2017.

1187 Duarte, H. F., Raczka, B. M., Ricciuto, D. M., Lin, J. C., Koven, C. D., Thornton, P. E.,  
1188 Bowling, D. R., Lai, C. T., Bible, K. J. and Ehleringer, J. R.: Evaluating the  
1189 Community Land Model (CLM4.5) at a coniferous forest site in northwestern United  
1190 States using flux and carbon-isotope measurements, *Biogeosciences*, 14(18): 4315-  
1191 4340, DOI: 10.5194/bg-14-4315-2017, 2017.

1192 Euskirchen, E.S., McGuire, A.D., Chapin, F.S. III, Yi, S., and Thompson, C.C.: Changes  
1193 in vegetation in northern Alaska under scenarios of climate change, 2003–2100:  
1194 implications for climate feedbacks, *Ecological Applications* 19: 1022-1043, 2009.

1195 Farquhar, G.D., von Caemmerer, S. and Berry, J.A.: A biochemical model of  
1196 photosynthetic CO<sub>2</sub> assimilation in leaves of C<sub>3</sub> species. *Planta*, 149, 78-90, 1980.

1197 [Fenner, N., Ostle, N.J., Mcnamara, N., Sparks, T., Harmens, H., Reynolds, B., and](#)  
1198 [Freeman, C.: Elevated CO<sub>2</sub> effects on peat- land plant community carbon dynamics](#)  
1199 [and DOC production, \*Ecosystem\*, 10,635-647,2007.](#)

1200 Frolking, S. and Roulet, N.T.: Holocene radiative forcing impact of northern peatland  
1201 carbon accumulation and methane emissions, *Glob. Change Biol.* 13, 1079-1088,  
1202 2007.

1203  
1204 [Frolking, S., Talbot, J., Jones, M. C., Treat, C. C., Kauffman, Tuittila E.-S., and Roulet,](#)  
1205 [N.: Peatlands in the Earth’s 21st century coupled climate-carbon system, \*Environ.\*](#)  
1206 [Rev.,19, 371-396, 2011.](#)

1207 Girardin, M. P., Bouriaud, O., Hogg, E. H., Kurz, W., Zimmermann, N. E., Metsaranta, J.  
1208 M., Jong, Rogier de, Frank, D. C., Esper, J., Büntgen, U., Guo, X., and Bhatti, J.: No  
1209 growth stimulation of Canada’s boreal forest under half-century of combined warming  
1210 and CO<sub>2</sub> fertilization, *Proceedings of the National Academy of Science*, 113(52),  
1211 E8406–E8414, 2016.

**Deleted:** Dise, N. B.: Peatland response to global change, *Science*, 326, 810- 811, <https://doi.org/10.1126/science.1174268>, 2009. ¶

**Formatted:** Normal (Web), Space Before: 0 pt, After: 0 pt

**Formatted:** Font: Times New Roman, 12 pt

**Formatted:** Font: Times New Roman, 12 pt

**Formatted:** Font: Times New Roman, 12 pt

**Formatted:** Font: Times New Roman, 12 pt

**Formatted:** Font: Times New Roman, 12 pt

**Field Code Changed**

**Formatted:** Hyperlink, Font: Times New Roman, 12 pt

**Formatted:** Font: Times New Roman, 12 pt

**Formatted:** Font: Do not check spelling or grammar

**Deleted:** Frolking, S., Roulet, N. T., Tuittila, E., Bubier, J. L., Quillet, A., Talbot, J., and Richard, P. J. H.: A new model of Holocene peatland net primary production, decomposition, water balance, and peat accumulation, *Earth Syst. Dynam.*, 1, 1-21, doi:10.5194/esd-1- 1-2010, 2010. ¶

- 1220 Goetz, J.D., and Price, J.S.: Role of morphological structure and layering of Sphagnum  
1221 and Tomenthypnum mosses on moss productivity and evaporation rates, Canadian  
1222 Journal of Soil Sciences. DOI:10.4141/ CJSS-2014-092, 2015.
- 1223 Golaz, J.-C., Caldwell, P. M., Van Roekel, L. P., Petersen, M. R., Tang, Q., Wolfe, J. D.,  
1224 Abeshu, G., Anantharaj, V., Asay-Davis, X. S., Bader, D.C., Baldwin, S. A., Bisht, G.,  
1225 Bogenschutz, P. A., Branstetter, M., Brunke, M., A., Brus, S.R., Burrows, S.M.,  
1226 Cameron-Smith P. J., Donahue, A. S., Deakin, M., Easter, R. C., Evans, K. J., Feng,  
1227 Y., Flanner, M., Foucar, J., G., Fyke, J. G., Griffin, B. M., Hannay, C., Harrop, B. E.,  
1228 Hoffman, M. J., Hunke, E. C., Jacob, R. L., Jacobsen, D. W., Jeffery, N., Jones, P. W.,  
1229 Klein, S. A., Larson, V. E., Leung, L. R., Li, H., Lin, W., Lipscomb, W.H., Ma, P.-L.,  
1230 Mahajan, S., Maltrud, M., E., Mamejtanov, A., McClean, J. L., McCoy, R. B., Neale,  
1231 R.B., Price, S. F., Qian, Y., Rasch, P. J., Reeves Eyre, J.E.J., Riley, W. J., Ringler, T.  
1232 D., Roberts, A. F., Roesler, E. L., Salinger, A. G., Shaheen, Z., Shi, X., Singh, B.,  
1233 Tang, J., Taylor, M. A., Thornton, P. E., Tuner, A. K., Veneziani, M., Wan, H., Wang,  
1234 H., Wang, S., Williams, D. N., Wolfram, P. J., Worley, P. H., Xie, S., Yang, Y., Yoon,  
1235 J.-H., Zelinka, M. D., Zender, C. S., Zeng, X., Zhang, C., Zhang, K., Zhang, Y.,  
1236 Zheng, X., Zhou, T., Zhu, Q.: The DOE E3SM coupled model version 1: Overview  
1237 and evaluation at standard resolution, *J. Adv. Model Earth Sy*, 11(7), 2089-2129,  
1238 <https://doi.org/10.1029/2018MS001603>, 2019.
- 1239 Gong, J., Roulet, N., Froking, S., Peltola, H., Laine, A.M., Kokkonen, N., and Tuittila,  
1240 E.-S.: Modelling the habitat preference of two key sphagnum species in a poor fen as  
1241 controlled by capitulum water retention, *Biogeosciences Discussions*,  
1242 <https://doi.org/10.5194/bg-2019-366>, 2019.
- 1243 Gorham, E.: Northern peatlands: role in the carbon cycle and probable responses to  
1244 climatic warming, *Ecological Applications*, 1, 182-195, 1991.
- 1245 Grant, R. F., Desai, A. R., and Sulman, B. N.: Modelling contrasting responses of  
1246 wetland productivity to changes in water table depth, *Biogeosciences*, 9, 4215-4231,  
1247 2012.
- 1248 Granath, G., Limpens, J., Posch, M., Muecher, S., and De Vries, W.: Spatio-temporal  
1249 trends of nitrogen deposition and climate effects on Sphagnum productivity in  
1250 European peatlands, *Environmental Pollution*, 187, 73-80, [https://doi.org/10.1016/j.](https://doi.org/10.1016/j.envpol.2013.12.023)  
1251 [envpol.2013.12.023](https://doi.org/10.1016/j.envpol.2013.12.023), 2014  
1252 Griffiths, N. A., and Sebastyen, S. D.: Dynamic vertical  
1253 profiles of peat porewater chemistry in a northern peatland, *Wetlands*, 36(6), 1119-  
1130, 2016.
- 1254 Griffiths, N. A., and Sebastyen, S. D.: Dynamic vertical profiles of peat porewater  
1255 chemistry in a northern peatland, *Wetland*, 36, 1119-1130, doi:10.1007/s13157-016-  
1256 0829-5, 2016.
- 1257 Griffiths, N. A., Hanson, P. J., Ricciuto, Iversen, C. M., Jensen, A.M., Malhotra, A.,  
1258 McFarlane, K. J., Norby, R. J., Sargsyan, K., Sebastyen, S. D., Shi, X., Walker, A. P.,  
1259 Ward, E. J., Warren, J. M., and Weston, D. J.: Temporal and spatial variation in  
1260 peatland carbon cycling and implications for interpreting responses of an ecosystem-  
1261 scale warming experiment, *Soil Sci. Soc. Am. J.*, 81(6), 1668-1688,  
1262 doi:10.2136/sssaj2016.12.0422, 2018.

1263 Grosvernier, P., Matthey, Y., and Buttler, A.: Growth potential of three Sphagnum  
1264 species in relation to water table level and peat properties with implications for their  
1265 restoration in cut-over bogs, Journal of Applied Ecology, 34(2), 471-483.  
1266 https://doi:10.2307/2404891,1997.

1267 Grosvernier, P.R., Mitchell, E.A.D., Buttler, A., Gobat, J.M.: Effects of elevated CO<sub>2</sub> and  
1268 nitrogen deposition on natural regeneration processes of cut-over ombrotrophic peat bogs  
1269 in the Swiss Jura mountains, Glob Change Prot Areas 9, 347-35, 2001.

1270 Gundale, M.J., DeLuca, T.H., and Nordin, A.: Bryophytes attenuate anthropogenic  
1271 nitrogen inputs in boreal forests, Glob. Change Biol.,17, 2743-2753, 2011.

1272 Gunnarsson, U., Granberg, G., & Nilsson, M.: Growth, production and interspecific  
1273 competition in *Sphagnum*: effects of temperature, nitrogen and sulphur treatments  
1274 on a boreal mire, *New Phytologist*, 163(2), 349-359, https://doi:10.1111/j.1469-  
1275 8137.2004.01108.x, 2004.

1276 Hanson, P. J., Riggs, J.S., Nettles, W. R., Krassovski, M. B., and Hook L. A.: SPRUCE  
1277 deep peat heating (DPH) environmental data, February 2014 through July 2015, Oak  
1278 Ridge National Laboratory, TES SFA, U.S. Department of Energy, Oak Ridge,  
1279 Tennessee, U.S.A. https://doi.org/10.3334/CDIAC/spruce.013, 2015a.

1280 Hanson, P.J., Riggs, J.S. Dorrance, C., Nettles, W.R., and Hook, L.A.: SPRUCE  
1281 Environmental Monitoring Data: 2010-2016. Carbon Dioxide Information Analysis  
1282 Center, Oak Ridge National Laboratory, U.S. Department of Energy, Oak Ridge,  
1283 Tennessee, U.S.A. http://dx.doi.org/10.3334/CDIAC/spruce.001, 2015b.

1284 Hanson, P. J., Gill, A. L., Xu, X., Phillips, J. R., Weston, D. J., Kolka, R. K., Riggs, J.  
1285 S., and Hook, L. A.: Intermediate-scale community-level flux of CO<sub>2</sub> and CH<sub>4</sub> in a  
1286 Minnesota peatland: putting the SPRUCE project in a global context,  
1287 Biogeochemistry, 129(3), 255-272, 2016.

1288 Hanson, P. J., Riggs, J.S., Nettles, W.R., Phillips, J.R., Krassovski, M.B., Hook, L.A.,  
1289 Gu, L., Richardson, A.D., Aubrecht, D.M., Ricciuto, D.M., Warren, J.M., and Barbier,  
1290 C.: Attaining whole-ecosystem warming using air and deep-soil heating methods with  
1291 an elevated CO<sub>2</sub> atmosphere, Biogeosciences, 14, 861-883, 2017.  
1292

1293 Hanson, P.J., Phillips, J.R., Wullschelger, S. D., Nettles, W. R., Warren, J. M., Ward, E.  
1294 J.: SPRUCE Tree Growth Assessments of Picea and Larix in S1-Bog Plots and  
1295 SPRUCE Experimental Plots beginning in 2011, Oak Ridge National Laboratory, TES  
1296 SFA, U.S. Department of Energy, Oak Ridge, Tennessee,  
1297 U.S.A. https://doi.org/10.25581/spruce.051/1433836, 2018a.  
1298

1299 Hanson, P.J., Phillips, J.R., Brice, D.J., and Hook, L.A.: SPRUCE Shrub-Layer Growth  
1300 Assessments in S1-Bog Plots and SPRUCE Experimental Plots beginning in  
1301 2010. Oak Ridge National Laboratory, TES SFA, U.S. Department of Energy, Oak  
1302 Ridge, Tennessee, U.S.A. https://doi.org/10.25581/spruce.052/1433837, 2018b.

1303 Hanson, P. J., Griffiths, N.A., Iversen, C.M., Norby, R. J., Sebestyen, S. D., Phillips,  
1304 Jeffrey, J. R., Chanton, P., Kolka, R. K., Malhotra, A., Oleheiser, K. C., Warren, J. M.,

Formatted: Normal, Indent: Left: 0", First line: 0", Space Before: Auto, After: Auto

Formatted: Font: Do not check spelling or grammar

Deleted: ¶

Formatted: EndNote Bibliography, Indent: Left: 0", Hanging: 0.5", Space After: 0 pt, Line spacing: single

Formatted: Font: (Default) Microsoft YaHei

Deleted: ¶

Formatted: Justified, Indent: Left: 0", Hanging: 0.25", No widow/orphan control, Don't adjust space between Latin and Asian text, Don't adjust space between Asian text and numbers

1307 [Shi, X., Yang, X., Mao, J., and Ricciuto, D. M.: Rapid net carbon loss from a whole-](#)  
1308 [ecosystem warmed peatland. \*AGU Advances\*, 1, e2020AV000163,](#)  
1309 <https://doi.org/10.1029/2020AV000163>, 2020.

1310 [Heijmans, M., Arp, W.J., Berendse, F.: Effects of elevated CO<sub>2</sub> and vascular plants on](#)  
1311 [evapotranspiration in bog vegetation, \*Glob Change Biol\* 7:817-827, 2001.](#)

1312 Heijmans, M.M.P.D., Arp, W.J., and Chapin, F.S. III.: Carbon dioxide and water vapour  
1313 exchange from understory species in boreal forest, *Agricultural and Forest*  
1314 *Meteorology* 123,135-147, DOI:10.1016/j. agrformet.2003.12.006, 2004a.

1315 Heijmans, M.M.P.D, Arp, W.J., and Chapin, F.S. III.: Controls on moss evaporation in a  
1316 boreal black spruce forest. *Global Biogeochemical Cycles* 18(2), 1-8,  
1317 DOI:10.1029/2003GB002128, 2004b.

1318 Heijmans, M.M. P. D., Mauquoy, D., van Geel, B., and Berendse, F.: Long-term effects  
1319 of climate change on vegetation and carbon dynamics in peat bogs. *Journal of*  
1320 *Vegetation Science* 19, 307-320, 2008.

1321 Hobbie, S.E., and Chapin, F.S. III.: The response of tundra plant biomass, aboveground  
1322 production, nitrogen, and CO<sub>2</sub> flux to experimental warming, *Ecology*, 79,1526-1544,  
1323 1998.

1324 Hobbie, S.E., Shevtsova, A., and Chapin, F.S.III.: Plant responses to species removal and  
1325 experimental warming in Alaskan Tus- sock Tundra. *Oikos* 84,417-434, 1999.

1326 [Hoosbeek, M.R., Van Breemen, N., Vasander, H., Buttler, A., Berendse, F.: Potassium](#)  
1327 [limits potential growth of bog vegetation under elevated atmospheric CO<sub>2</sub> and N](#)  
1328 [deposition, \*Glob. Change Biol.\*, 8,1130-1138, https://doi. org/10.1046/j.1365-](#)  
1329 [2486.2002.00535.x](https://doi.org/10.1046/j.1365-2486.2002.00535.x), 2002.

1330 Ise, T., Dunn, A. L., Wofsy, S. C., and Moorcroft, P. R.: High sensitivity of peat  
1331 decomposition to climate change through water table feedback, *Nat. Geosci.*, 1, 763-  
1332 766, 2008.

1333 [Jauhiainen, J., Silvola, J.: Photosynthesis of \*Sphagnum fuscum\* at long-term raised CO<sub>2</sub>](#)  
1334 [concentrations, \*Annales Botanici Fennici\*, 36,11-19, 1999.](#)

1335 Jensen, A.M., Warren, J. M., Hook, L. A., Wullschlegler, S. D., Brice, D.J., Childs, J.,  
1336 and Vander Stel, H.M.: SPRUCE S1 Bog Pretreatment Seasonal Photosynthesis and  
1337 Respiration of Trees, Shrubs, and Herbaceous Plants, 2010-2015, Oak Ridge National  
1338 Laboratory, TES SFA, U.S. Department of Energy, Oak Ridge, Tennessee, U.S.A.,  
1339 <https://doi.org/10.3334/CDIAC/spruce.008>, 2018.

1340 Jensen, A.M., Warren, J. M., King, A., Ricciuto, D.M., Hanson, P. J., and Wullschlegler,  
1341 S. D.: Simulated projections of boreal forest peatland ecosystem productivity are  
1342 sensitive to observed seasonality in leaf phenology, *Tree Physiology*, 39(4), 556-572,

Formatted: Space Before: Auto, After: Auto

Formatted: Subscript

Formatted: Font: Do not check spelling or grammar

Formatted: Indent: Left: 0", First line: 0"

Formatted: Font: Do not check spelling or grammar

Formatted: Indent: Left: 0", First line: 0"

Formatted: Font: Do not check spelling or grammar

Formatted: Space After: 12 pt, No widow/orphan control, Don't adjust space between Latin and Asian text, Don't adjust space between Asian text and numbers

- 1343 doi: 10.1093/treephys/tpy140, 2019.
- 1344 Jiang, J., Huang, Y., Ma, S., Stacy, M., Shi, Z., Ricciuto, D. M., Hanson, P. J., and Luo,  
1345 Y.: Forecasting Responses of a Northern Peatland Carbon Cycle to Elevated CO<sub>2</sub> and  
1346 a Gradient of Experimental Warming, *J. Geophys. Res.-Biogeo*, 123(3), 1057-1071,  
1347 doi: 10.1002/2017JG004040, 2018.
- 1348 Juday, G. P., and Alix, C.: Consistent negative temperature sensitivity and positive  
1349 influence of precipitation on growth of floodplain *Picea glauca* in Interior Alaska,  
1350 *Canadian Journal of Forest Research*, 42, 561-573, 2012.
- 1351 Kostka, J.E., Weston, D.J., Glass, J.B., Lilleskov, E.A., Shaw, A.J., and Turetsky, M.R.:  
1352 The Sphagnum microbiome: new insights from an ancient plant lineage, *New*  
1353 *Phytologist*, 211(1):57-64, 2016
- 1355 Kuiper, J. J., Mooij, W. M., Bragazza, L., and Robroek, B. J.: Plant functional types  
1356 define magnitude of drought response in peatland CO<sub>2</sub> exchange, *Ecology*, 95, 123-  
1357 131, <https://doi.org/10.1890/13-0270.1>, 2014.
- 1358 Lafleur, P. M., Hember, R. A., Admiral, S. W., and Roulet, N. T.: Annual and seasonal  
1359 variability in evapotranspiration and water table at a shrub-covered bog in southern  
1360 Ontario, Canada, *Hydrol. Process.*, 19, 3533–3550, <https://doi.org/10.1002/hyp.5842>,  
1361 2005.
- 1362 [Larmola, T., Leppänen, S. M., Tuittila, E.-Stiina, Aarva, M., Merilä, P., Fritze, H.,](#)  
1363 [Tiirola, M.: Methanotrophy induces nitrogen fixation during peatland development,](#)  
1364 [PNAS. 734-739, www.pnas.org/cgi/dio/10.1073/pnas.1314284111, 2014.](#)
- 1365 Launiainen, S., Katul, G. G., Lauren, A., and Kolari, P.: Coupling boreal forest CO<sub>2</sub>, H<sub>2</sub>O  
1366 and energy flow by a vertically structured forest canopy-Soil model with separate  
1367 bryophyte layer. *Ecological Modelling*, 312, 385-405.  
1368 <https://doi.org/10.1016/j.ecolmodel.2015.06.007>, 2015.
- 1369 Limpens, J., Berendse, F., Blodau, C., Canadell, J. G., Freeman, C., Holden, J., Roulet,  
1370 N., Rydin, H., and Schaepman-Strub, G.: Peatlands and the carbon cycle: From local  
1371 processes to global implications-A synthesis, *Biogeosciences*, 5(5), 1475-1491,  
1372 doi:10.5194/bg-5-1475-2008, 2008.
- 1373 Lindo, Z., and Gonzalez, A.: The bryosphere: an integral and influential component of the  
1374 earth's biosphere, *Ecosystems*, 13, 612–627, 2010.
- 1375 Lindo, Z., Nilsson, M.C., and Gundale, M.J.: Bryophyte-cyanobacteria associations as  
1376 regulators of the northern latitude carbon balance in response to global change, *Glob.*  
1377 *Change Biol.*, 19(7),2022-35, 2013.
- 1378 Lu, D., Ricciuto, D.M., Stoyanov, M., and Gu, L.: Calibration of the E3SM Land Model  
1379 Using Surrogate-Based Global Optimization, *J Adv Model Earth Sy*, 10(6), 1337-  
1380 1356, doi: 10.1002/2017ms001134, 2018.

Deleted: ¶

Deleted: ¶

Formatted: Indent: Left: 0", First line: 0"

Formatted: Normal (Web), Space Before: 0 pt, After: 0 pt

Formatted: Font: Times New Roman, 12 pt

Formatted: Font: Times New Roman, 12 pt



- 1383 Lu, D., and Ricciuto, D.M.: Efficient surrogate modeling methods for large-scale Earth  
1384 system models based on machine-learning techniques, *Geosci Model Dev*, 12(5),  
1385 1791-1807, doi: 10.5194/gmd-12-1791-2019, 2019.
- 1386 Man, R., Kayahara, G.J., Rice, J.A., and MacDonald, G.B.: Eleven- year responses of a  
1387 boreal mixedwood stand to partial har- vesting: light, vegetation, and regeneration  
1388 dynamics, *For Ecol Manag* 255,697-706, 2008.
- 1389 Mazziotta, A., Granath, G., Rydin, H. and Bengtsson F.: Scaling functional traits to  
1390 ecosystem processes: Towards a mechanistic understanding in peat mosses, *Journal of*  
1391 *Ecology*, DOI:10.1111/1365-2745.13110, 2018.
- 1392 Metcalfe, D. B., Ricciuto D. M., Palmroth, S., Campbell, Hurry, C., V., Mao, J., Keel, S.  
1393 G., Linder, S., Shi, X., Näsholm, T., Ohlsson, K. E. A., Blackburn, M., Thornton, P. E.  
1394 and Oren, R.: Informing climate models with rapid chamber measurements of forest  
1395 carbon uptake, *Global Change Biology*, 23(5), 2130-2139, DOI: 10.1111/gcb.13451,  
1396 2017.
- 1397 McFadden, J.P., Eugster, W., Chapin, F.S.III.: A regional study of the controls on water  
1398 vapor and CO2 exchange in Arctic tundra, *Ecology*, 84,2762-76, 2003.
- 1399 McGuire, A. D., Anderson, L. G., Christensen, T. R., Dallimore, S., Guo, L., Hayes, D.  
1400 J., Heimann, M., Lorenson, T. D., Macdonald, R. W. and Roulet, N.: Sensitivity of the  
1401 carbon cycle in the Arctic to climate change, *Ecol. Monogr.*, 79, 523-555, 2009.
- 1402 Miller, P. A. and Smith, B.: Modelling Tundra Vegetation Response to Recent Arctic  
1403 Warming, *Ambio*, 41, 281-291, <https://doi.org/10.1007/s13280-012-0306-1>, 2012.
- 1404 Mokhov, I.I., Eliseev, A.V., and Denisov, S.N.: Model diagnostics of variations in  
1405 methane emissions by wetlands in the second half of the 20th century based on  
1406 reanalysis data, *Dokl. Earth Sci.*, 417(1),1293-1297, 2007.
- 1407 Moore, T.R., Roulet, N.T., and Waddington, J.M.: Uncertainty in predicting the effect of  
1408 climate change on the carbon cycling of Canadian peatlands, *Clim. Change*, 40, 229-  
1409 245, 1998.
- 1410 Myneni, R. B., Keeling, C. D., Tucker, C. J., Asrar, G., and Nemani, R. R.: Increased  
1411 plant growth in the northern high latitudes from 1981 to 199,1 *Nature*, 386,698-702,  
1412 1997.
- 1413 Murray, K.J., Tenhunen, J.D., and Nowak, R.S.: Photoinhibition as a control on  
1414 photosynthesis and production of Sphagnum mosses, *Oecologia*, 96,200-207, 1993.
- 1415 Nichols, J.E., and Peteet, D.M.: Rapid expansion of northern peatlands and doubled  
1416 estimate of carbon storage, *Nat. Geosci.* 12, 917-921, doi:10.1038/s41561-019-0454-z,  
1417 2019.

1418 Nilsson, M.C., and Wardle, D.A.: Understory vegetation as a forest ecosystem driver:  
1419 evidence from the northern Swedish boreal forest, *Frontiers in Ecology and the*  
1420 *Environment*, 3, 421-428, 2005.

1421 Norby, R.J., and Childs, J.: Sphagnum productivity and community composition  
1422 in the SPRUCE experimental plots. Carbon Dioxide Information Analysis  
1423 Center, Oak Ridge National Laboratory, U.S. Department of Energy, Oak  
1424 Ridge, Tennessee, U.S.A. <http://dx.doi.org/10.3334/CDIAC/spruce.xxx>, 2017.

1425 Norby, R.J., Childs, J., Hanson, P.J., and Warren, J.M.: Rapid loss of an ecosystem  
1426 engineer: Sphagnum decline in an experimentally warmed bog, *Ecology and*  
1427 *Evolution*, 9(22), 12571-12585, <https://doi.org/10.1002/ece3.5722>, 2019.

1428 Nungesser, M. K.: Modelling microtopography in boreal peatlands: Hummocks and  
1429 hollows, *Ecol. Model.*, 165(2-3), 175-207, 2003.

1430

1431 Oechel, W.C., and Van Cleve, K.: The role of bryophytes in nutrient cycling in the taiga,  
1432 in *Ecological Studies*, Vol. 57: Forest Ecosystems in the Alaskan Taiga, edited by:  
1433 Van Cleve, K., Chapin III, F. S., Flanagan, P.W., Viereck, L.A., and Dyrness, C.T.,  
1434 Springer-Verlag, New York, 121-137, 1986.

1435 Oleson, K. W., Lawrence, D. W., Bonan, G. B., Drewniak, B., Huang, M., Koven, C. D.,  
1436 Levis, S., Li, F., Riley, W. J., Subin, Z. M., Swenson, S. C., Thornton, P. E., Bozbiyik,  
1437 A., Fisher, R., Heald, C. L., Kluzek, E., Lamarque, J., Lawrence, P. J., Leung, L. R.,  
1438 Lipscomb, W., Muszala, S., Ricciuto, D. M., Sacks, W., Sun, Y., Tang, J., and Yang,  
1439 Z.: Technical description of version 4.5 of the Community Land Model (CLM),  
1440 NCAR/TN-503+STR, NCAR Technical Note, 2013.

1441 Park, H., Launiainen, S., Konstantinov, P. Y., Iijima, Y., and Fedorov, A. N.: Modeling  
1442 the effect of moss cover on soil temperature and carbon fluxes at a tundra site in  
1443 northeastern Siberia, *J. Geophys. Res.-Bioge*, 123, 3028-3044, <https://doi.org/10.1029/2018JG004491>, 2018.

1444

1445 Parsekian, A. D., Slater, L., Ntarlagiannis, D., Nolan, J., S. Sebestyen, D., Kolka, R. K.,  
1446 and Hanson, P. J.: Uncertainty in peat volume and soil carbon estimated using ground-  
1447 penetrating radar and probing. *Soil Sci. Soc. Am. J.*, 76, 1911-1918. DOI:  
1448 [10.2136/sssaj2012.0040](https://doi.org/10.2136/sssaj2012.0040), 2012.

1449 Pastor, J., Peckham, B., Bridgham, S., Weltzin, J., and Chen, J.: Plant community  
1450 dynamics, nutrient cycling, and alternative stable equilibria in peatlands, *The*  
1451 *American Naturalist* 160, 553-568, 2002.

1452 Peichl, M., Öquist, M., Löfvenius, M. O., Ilstedt, U., Sagerfors, J., Grelle, A., Lindroth,  
1453 A., and Nilsson, M. B.: A 12-year record reveals pre-growing season temperature and  
1454 water table level threshold effects on the net carbon dioxide exchange in a boreal fen,  
1455 *Environ. Res. Lett.*, 9, 055006, <https://doi.org/10.1088/1748-9326/9/5/055006>, 2014.

1456 Petrone, R., Solondz, D., Macrae, M., Gignac, D., and Devito, K.J.: Microtopographical  
1457 and canopy cover controls on moss carbon dioxide exchange in a western boreal plain  
1458 peatland, *Ecohydrology*, 4, 115-129, 2011.

1459 [Porada, P., Weber, B., Elbert, W., Pöschl, U., and Kleidon, A.: Estimating global carbon](#)  
1460 [uptake by lichens and bryophytes with a process-based model, \*Biogeosciences\*, 10,](#)  
1461 [6989–7033, doi:10.5194/bg-10-6989-2013, 2013.](#)

1462 [Porada, P., Ekici, A., and Beer, C.: Effects of bryophyte and lichen cover on permafrost](#)  
1463 [soil temperature at large scale, \*The Cryosphere\*, 10\(5\), 2291–2315,](#)  
1464 <https://doi.org/10.5194/tc-10-2291-2016>, 2016.

1465 Raczka, B., Duarte, H. F., Koven, C. D., Ricciuto, D.M., Thornton, P. E., Lin, J. C. and  
1466 Bowling, D. R.: An observational constraint on stomatal function in forests: evaluating  
1467 coupled carbon and water vapor exchange with carbon isotopes in the Community  
1468 Land Model (CLM4.5), *Biogeosciences*, 13(18), 5183-5204, DOI: 10.5194/bg-13-  
1469 5183-2016, 2016.

1470 Raghoebarsing, A. A., Smolders, A.J.P., Schmid, M.C., Rijpstra, W.I.C., Wolters-Arts,  
1471 M., Derksen, J., Jetten, M.S.M., Schouten, S., Sinninghe Damsté, J.S., Lamers,  
1472 L.P.M., Roelofs, J.G.M., Op den Camp, H.J.M., and Strous, M.: Methanotrophic  
1473 symbionts provide carbon for photosynthesis in peat bogs. *Nature*, 436, 1153-1156,  
1474 doi:10.1038/nature03802, 2005.

1475

1476 Ricciuto, D. M., Sargsyan, K., and Thornton, P.E.: The Impact of Parametric  
1477 Uncertainties on Biogeochemistry in the E3SM Land Model, *J Adv Model Earth Sy*,  
1478 10(2), 297-319, doi: 10.1002/2017ms000962, 2018.

1479 Ricciuto, D.M., Xu, X., Shi, X., Wang, Y., Song, X., Schadt, C.W., Griffiths, N. A., Mao,  
1480 J., Warre, J.,M., Thornton, P.E., Chanton, J., Keller, J., Bridgham, S., Gutknecht, J.,  
1481 Sebestyen, S. D., Finzi, A., Kolka, R., and Hanson P.J.: An Integrative Model for Soil  
1482 Biogeochemistry and Methane Processes: I. Model Structure and Sensitivity Analysis,  
1483 *J. Geophys. Res.-Biogeo*, In review, 2019.

1484 Riutta, T., Laine, J., and Tuittila, E.-S.: Sensitivity of CO<sub>2</sub> exchange of fen ecosystem  
1485 componetns to water level variation, *Ecosystem*, 10(5), 718-733, 2007.

1486 Robroek, B.J.M., Limpens, J., Breeuwer, A., and Schouten, M.G.C.: Effects of water  
1487 level and temperature on performance of four Sphagnum mosses. *Plant*  
1488 *Ecology*, 190, 97-107, 2007.

1489 Robroek, B.J.M., Schouten, M.G.C., Limpens, J., Berendse F. and Poorter, H.: Interactive  
1490 effects of water table and precipitation on net CO<sub>2</sub> assimilation of three co-occurring  
1491 Sphagnum mosses differing in distribution above the water table, *Glob. Change Biol.*,  
1492 15, 680-691, 2009.

1493 Rosenzweig, C., Karoly, D., Vicarelli, M., Neofotis, P., Wu, Q., Casassa, G., Menzel, A.,  
1494 Root, T., Estrella, N., Seguin, B., Tryjanowski, P., Liu, C., Ravlins, S., and Imeson,  
1495 A.: Attributing physical and biological impacts to anthropogenic climate  
1496 change, *Nature*, 453, 353-357, doi:10.1038/nature06937, 2008.

1497 [Rydin, H.: Effect of water level on desiccation of Sphagnum in relation to surrounding](#)  
1498 [Sphagna, \*Oikos\*, 45\(3\), 374-379, https://doi:10.2307/3565573, 1985.](#)

Formatted: Font: Times New Roman, 12 pt

Formatted: Indent: Left: 0", Hanging: 0.19"

Formatted: Font: Times New Roman, 12 pt

Formatted: Font: Times New Roman, 12 pt

Formatted: Font: Times New Roman, 12 pt

Field Code Changed

Formatted: Hyperlink, Font: Times New Roman, 12 pt

Formatted: Font: Times New Roman, 12 pt

- 1499 [Rydin, H., and Clymo, R. S.: Transport of carbon and phosphorus-compounds about](#)  
1500 [Sphagnum. Proceedings of the Royal Society Series B-Biological Sciences,](#)  
1501 [237\(1286\), 63-84. <https://doi.org/10.1098/rspb.1989.0037>, 1989.](#)
- 1502 Rousk, K., Rousk, J., Jones, D.L., Zackrisson, O., DeLuca, and T.H.: Feather moss  
1503 nitrogen acquisition across natural fertility gradients in boreal forests, *Soil Biol*  
1504 *Biochem*, 61, 86-95, 2013.
- 1505 Rousk, K., and Michelsen, A.: The sensitivity of Moss-Associated Nitrogen Fixtion  
1506 towards Repeated Nitrogen Input, *Plos One*, 11(1), e0146655,  
1507 <https://doi.org/10.1371/journal.pone.0146655>, 2016.
- 1508 Rydsaa, J. H., Stordal, F., Bryn, A., and Tallaksen, L. M.: Effects of shrub and tree cover  
1509 increase on the near-surface atmosphere in northern Fennoscandia, *Biogeosciences*,  
1510 14, 4209-4227, <https://doi.org/10.5194/bg-14-4209-2017>, 2017.
- 1511 [Saamio, S., Jarvio, S., Saarinen, T., Vasander, H., Silvola, J.: Minor changes in](#)  
1512 [vegetation and carbon gas balance in a boreal mire under a raised CO<sub>2</sub> or](#)  
1513 [NH<sub>4</sub>NO<sub>3</sub> supply, \*Ecosystems\* 6:46-60, \[https://doi.org/10.1007/s10021-002-\]\(https://doi.org/10.1007/s10021-002-0208-3\)  
1514 \[0208-3\]\(#\), 2003.](#)
- 1515 Sargsyan, K., Safta, C., Najm, H. N., Debusschere, B. J., Ricciuto, D.M., and Thornton,  
1516 P.E.: Dimensionality Reduction for Complex Models Via Bayesian Compressive  
1517 Sensing, *International Journal for Uncertainty Quantification*, 4(1), 63-93, doi:  
1518 10.1615/Int.J.UncertaintyQuantification.2013006821, 2014.
- 1519 Sebestyen, S. D., Dorrance, C., Olson, D. M., Verry, E. S., Kolka, R. K., Elling, A. E.,  
1520 and Kyllander, R.: Long-term monitoring sites and trends at the Marcell Experimental  
1521 Forest, in: *Peatland biogeochemistry and watershed hydrology at the Marcell*  
1522 *Experimental Forest*, edited by: Kolka, R. K. Sebestyen, S. D., Verry, E. S., and  
1523 Brooks, CRC Press, New York, 15-71, 2011.
- 1524 Shi, X., Thornton, P. E., Ricciuto, D. M., Hanson, P. J., Mao, J., Sebestyen, S. D.,  
1525 Griffiths, N. A., and Bisht, G.: Representing northern peatland microtopography and  
1526 hydrology within the Community Land Model, *Biogeosciences*, 12(21), 6463-6477,  
1527 <https://doi.org/10.5194/bg-12-6463-2015>, 2015.
- 1528 Silva, L. C. R., Anand, M., and Leithead, M. D.: Recent widespread tree growth decline  
1529 despite increasing atmospheric CO<sub>2</sub>, *PLoS ONE*, 5(7), e11543, doi:  
1530 10.1371/journal.pone.0011543, 2010.
- 1531
- 1532 Sonnentag, O., Van Der Kamp, G., Barr, A.G., and Chen, J.: on the relationship between  
1533 water table depth and water vapor and carbon dioxide fluxes in a minerotrophic fen,  
1534 *Glob. Change Biol.*, 16(6), 1761-1776, [https://doi.org/10.1111/j.1365-](https://doi.org/10.1111/j.1365-2486.2009.02032.x)  
1535 [2486.2009.02032.x](#), 2010.
- 1536 St-Hilaire, F., Wu, J., Roulet, N. T., Frohking, S., Lafleur, P. M., Humphreys, E. R., and  
1537 Arora, V.: McGill wetland model: evaluation of a peatland carbon simulator  
1538 developed for global assessments, *Biogeosciences*, 7, 3517-3530, 2010.
- 1539 Sulman, B. N., Desai, A. R., Saliendra, N. Z., Lafleur, P. M., Flanagan, L. B.,  
1540 Sonnentag, O., Mackay, D. S., Barr, A. G., and Kamp, G. V. D.: CO<sub>2</sub> fluxes at

Deleted: ¶

Rydin, H., and Jeglum, J.: *The Biology of Peatlands*, 343 pp., Oxford University Press, New York, 2006. ¶

Formatted: EndNote Bibliography, Indent: Left: 0", Hanging: 0.5"

Deleted: ¶

1545 northern fens and bogs have opposite responses to inter-annual fluctuations in water  
1546 table, *Geophys. Res. Lett.*, 37, L19702, doi:10.1029/2010GL044018, 2010.

1547 Tarnocai, C.: The effect of climate change on carbon in Canadian peatlands, *Glob Planet*  
1548 *Change*, 53, 4, 222-232, 2006.

1549 Tenhunen, J.D., Weber, J.A., Yocum, C.S. and Gates, D.M.: Development of a  
1550 photosynthesis model with an emphasis on ecological applications, *Oecologia*, 26, 101-  
1551 119, 1976.

1552  
1553 Tian, H., Lu, C., Yang, J., Banger, K., Huntinzger, D. N., Schwalm, C. R., Michalak, A.  
1554 M., Cook, R., Ciais, P., Hayes, D., Huang, M., Ito, A., Jacobson, A., Jain, A., Lei, H.,  
1555 Mao, J., Pan, S., Post, W.M, Peng, S., Poulter, B., Ren, W., Ricciuto, D.M., Schaefer, K.,  
1556 Shi, X., Tao, B., Wang, W., Wei, Y., Yang, Q., Zhang, B., and Zeng, N.: Global patterns  
1557 of soil carbon stocks and fluxes as simulated by multiple terrestrial biosphere models:  
1558 sources and magnitude uncertainty, *Global Biogeochem Cycles*, 29, 775-792,  
1559 doi:10.1002/2014GB005021, 2015.

1560 Titus, J. E., Wagner, D.J., and Stephens, M.D.: Contrasting Water Relations of  
1561 Photosynthesis for 2 Sphagnum Mosses, *Ecology*, 64, 1109-1115, 1983.

1562 Todd-Brown, K. E. O., Randerson, J. T., Post, W. M., Hoffman, F. M., Tarnocai, C.,  
1563 Schuur, E. A. G., and Allison, S. D.: Causes of variation in soil carbon simulations  
1564 from CMIP5 Earth system models and comparison with observations, *Biogeosciences*,  
1565 10, 1717-1736, doi:10.5194/bg-10-1717-2013, 2013.

1566 Toet, S., Cornelissen, J.H., Aerts, R., van Logtestijn, R.S., de Beus, M., Stoevelaar, R.:  
1567 Moss responses to elevated CO<sub>2</sub> and variation in hydrology in a temperate lowland  
1568 peatland. *Plants and climate change*. Springer, Netherlands, pp 27-42, 2006.

1569 Turetsky, M. R., Wieder, R. K., and Vitt, D. H.: Boreal peatland C fluxes under varying  
1570 permafrost regimes, *Soil Biol. Biochem.*, 34, 907-912, 2002.

1571 Turetsky, M. R., and Wieder, R. K.: Boreal bog Sphagnum refixes soil-produced and  
1572 respired 14CO<sub>2</sub>. *Ecoscience*, 6(4), 587-591.  
1573 [https://doi:10.1080/11956860.1999.11682559](https://doi.org/10.1080/11956860.1999.11682559), 1999.

1574 Turetsky, M.R., Mack, M.C., Hollingsworth, T.N., and Harden, J.W.: The role of mosses  
1575 in ecosystem succession and function in Alaska's boreal forest, *Canadian Journal of*  
1576 *Forest Research* 4, 1237-1264, 2010.

1577 Turetsky, M. R., Bond-Lamberty, B., Euskirchen, E., Talbot, J., Frohling, S., McGuire,  
1578 A. D., and Tuittila, E.-S.: The resilience and functional role of moss in boreal and arctic  
1579 ecosystems, *New Phytol.*, 196, 49-67, doi:10.1111/j.1469- 8137.2012.04254.x,  
1580 2012.

1581  
1582 Van, B. N.: How Sphagnum bogs down other plants, *Trends Ecol. Evol*, 10, 270-275,  
1583 1995.

1584 Van Der Heijden, E., Verbeek, S.K., Kuiper, P.J.C.: Elevated atmospheric CO<sub>2</sub> and  
1585 increased nitrogen deposition: effects on C and N metabolism and growth of the peat

Deleted: .

Deleted: ¶

Formatted: Font: Do not check spelling or grammar

Deleted: ¶

Formatted: Indent: Left: 0", First line: 0", Space Before: Auto, After: Auto

1589 [moss \*Sphagnum recurvum\* P. Beauv. var. \*mucronatum\* \(Russ.\), Warnst. \*Glob Change\*](#)  
1590 [Biol 6, 201-212, <https://doi.org/10.1046/j.1365-2486.2000.00303.x>, 2000.](#)

1591 van der Schaaf, S.: Bog hydrology, in: Conservation and Restoration of Raised Bogs:  
1592 Geological, Hydrological and Ecological Studies, edited by: Schouten, M.G.C., The  
1593 Government Stationery Office, Dublin, 54-109, 2002.

1594 van der Wal, R., Pearce, I.S.K and Brooker, R.W.: Mosses and the struggle for light in a  
1595 nitrogen-polluted world, *Oecologia*, 142,159-68, 2005.

1596 [Van Gaalen, K. E., Flanagan, L. B., and Peddle, D. R.: \*Photosynthesis, chlorophyll\*](#)  
1597 [fluorescence and spectral reflectance in \*Sphagnum\* moss at varying water contents,](#)  
1598 [Oecologia, 153\(1\), 19-28, doi:10.1007/s00442-007-0718-y, 2007.](#)

1599 Verry, E. S., and Janssens, J.: Geology, vegetation, and hydrology of the S2 bog at the  
1600 MEF: 12,000 years in northern Minnesota, in Peatland biogeochemistry and watershed  
1601 hydrology at the Marcell Experimental Forest, edited by R. K. Kolka S. D.  
1602 Sebestyen, E. S. Verry, K.N. Brooks, CRC Press, New York, 93-134, 2011.

1603 Vile, M. A., Kelman Wieder, R., Živković, T., Scott, K. D., Vitt, D. H., Hartsock, J. A.,  
1604 Iosue, C. L., Quinn, J.C., Petix, M., Fillingim, H.M., Popma, J.M.A., Dynarski, K.A.,  
1605 Jackman, T. R., Albright, C.M., and Wykoff, D. D. : N<sub>2</sub>-fixation by methanotrophs  
1606 sustains carbon and nitrogen accumulation in pristine peatlands, *Biogeochemistry*,  
1607 121, 317-328, <https://doi.org/10.1007/s10533-014-0019-6>, 2014.

1608 Vitt, D. H.: A key and review of bryophytes common in North American peatlands,  
1609 *Evansia*, 31, 121-158, 2014.

1610 Wania, R., Ross, I., Prentice, I.C.: Integrating peatlands and permafrost into a dynamic  
1611 global vegetation model: 1. Evaluation and sensitivity of physical land surface  
1612 processes, *Global Biogeochem. Cycles* 23, GB3014, doi:10.1029/2008GB003412,  
1613 2009.

1614 Wania, R., Melton, J. R., Hodson, E. L., Poulter, B., Ringeval, B., Spahni, R., Bohn, T.,  
1615 Avis, C. A., Chen, G., Eliseev, A. V., Hopcroft, P. O., Riley, W. J., Subin, Z. M., Tian,  
1616 H., van Bodegom, P.M., Kleinen, T., Yu, Z., Singarayer, J. S., Zurcher, S.,  
1617 Lettenmaier, D. P., Beerling, D. J., Denisov, S. N., Prigent, C., Papa, F., and Kaplan, J.  
1618 O.: Present state of global wetland extent and wetland methane modelling:  
1619 methodology of a model inter-comparison project (WETCHIMP), *Geosci. Model*  
1620 *Dev.*, 6, 617-641, 2013.

1621 Walker, M.D., Wahren, C.H., Hollister, R.D., Henry, G.H.R., Ahlquist, L.E., Alatalo,  
1622 J.M., Bret-Harte, M.S., Calef, M.P., Callaghan, T.V., Carroll, A.B., Epstein, H.E.,  
1623 Jonsdottir, I.S., Klein, J.A., Magnusson, B., Molau, U., Oberbauer, S.F., Rewa, S.P.,

Deleted: ¶

Formatted: EndNote Bibliography, Indent: Left: 0", Hanging: 0.25", Space Before: 0 pt, After: 0 pt, Line spacing: Double

Formatted: Font: (Default) Times New Roman, Not Italic

Formatted: Font: (Default) Times New Roman, Not Italic

Formatted: Comment Text

Deleted: ¶

- 1626 Robinson, C.H., Shaver, G.R., Suding, K.N., Thompson, C.C., Tolvanen, A., Totland,  
1627 O., Turner, P.L., Tweedie, C.E., Webber, and P.J., Wookey, P.A.: Plant community  
1628 responses to experimental warming across the tundra biome, *Proc Natl Acad Sci USA*,  
1629 10,31342-6, 2006.
- 1630 Walker, T. N., Ward, S. E., Ostle, N. J., and Bardgett, R. D.: Contrasting growth  
1631 responses of dominant peatland plants to warming and vegetation composition,  
1632 *Oecologia*, 178, 141-151, <https://doi.org/10.1007/s00442-015-3254-1>, 2015.
- 1633 Walker, A. P., Carter, K. R., Gu, L., Hanson, P. J., Malhotra, A., Norby, R.J., Sebestyen,  
1634 S. D., Wullschleger, S. D., Weston, D. J.: 2017. Biophysical drivers of seasonal  
1635 variability in Sphagnum gross primary production in a northern temperate bog, *J.*  
1636 *Geophys. Res.-Biogeo*, 122, 1078-1097, <https://doi.org/10.1002/2016JG003711>, 2017.
- 1637 Wang, H., Richardson, C. J., and Ho, M.: Dual controls on carbon loss during drought in  
1638 peatlands, *Nature Climate Change*, 5, 58- 587, 2015.
- 1639 Ward, S. E., Ostle, N. J., Oakley, S., Quirk, H., Henrys, P. A., and Bardgett, R. D.:  
1640 Warming effects on greenhouse gas fluxes in peatlands are modulated by vegetation  
1641 composition, *Ecol. Lett.*, 16, 1285-1293, 2013.
- 1642 [Weltzin, J. F., Harth, C., Bridgham, S. D., Pastor, J., and Vonderharr, M.: Production and](#)  
1643 [microtopography of bog bryophytes: response to warming and water-table](#)  
1644 [manipulations, \*Oecologia\*, 128\(4\), 557-565, https://doi:10.1007/s004420100691,](#)  
1645 [2001.](#)
- 1646 [Weston, D.J., Timm, C.M., Walker, A.P., Gu, L., Muchero, W., Schmuta, J., Shaw, A. J.,](#)  
1647 [Tuskan, G. A., Warren, J.M., and Wllschleger, S.D.: Sphagnum physiology in the](#)  
1648 [context of changing climate: Emergent influences of genomics, modeling and host-](#)  
1649 [microbiome interactions on understanding ecosystem function, \*Plant, Cell and\*](#)  
1650 [Environment, 38, 1737-1751, doi: 10.1111/pce.12458, 2015.](#)
- 1651 White, M. A., Thornton, P. E., Running, S. W., and Nemani, R. R.: Parameterization and  
1652 sensitivity analysis of the BIOME-BGC terrestrial ecosystem model: Net primary  
1653 production controls, *Earth Interactions*, 4(3), 1-85, 2000.
- 1654 Wieder R. K.: Primary production in boreal peatlands. In: *Boreal peatland ecosystems*,  
1655 edited by: Wieder, R. K., and Vitt, D. H., Springer-Verlag, Berlin Heidelberg,  
1656 Germany, 145-163, 2006.
- 1657 Wiley, E., Rogers, B. J., Griesbauer, H. P., and Landhausser, S. M.: Spruce shows greater  
1658 sensitivity to recent warming than Douglas-fir in central British Columbia, *Ecosphere*  
1659 9(5), e02221, [10.1002/ecs2.2221](https://doi.org/10.1002/ecs2.2221), 2018Williams T.G. and Flanagan, L.B.: Measuring

Formatted: Indent: Left: 0", Hanging: 0.25"

Deleted: ¶

- 1661 and modelling environmental influences on photosynthetic gas exchange in Sphagnum  
1662 and Pleurozium, *Plant Cell and Environment*, 21, 555-564, 1998.
- 1663 [Williams T.G. & Flanagan L.B.: Measuring and modelling environmental influences on](#)  
1664 [photosynthetic gas exchange in \*Sphagnum\* and \*Pleurozium\*, \*Plant Cell and\*](#)  
1665 [Environment, 21, 555-564,1998.](#)
- 1666 Wilmking, M., Juday, G. P., Barber, V. A., and Zald, H. S. J.: Recent climate warming  
1667 forces contrasting growth responses of white spruce at treeline in Alaska through  
1668 temperature thresholds, *Glob. Change Biol.* 10,1724-1736, 2004.
- 1669 Wolf, A., Callaghan, T. V., and Larson, K.: Future changes in vegetation and ecosystem  
1670 function of the Barents Region, *Climatic Change*, 87, 51-73,  
1671 <https://doi.org/10.1007/s10584-007-9342-4>, 2008.
- 1672 Wolken, J. M., Mann, D. H., Grant, T. A., Lloyd, A. H., Rupp, T.S., and Hollingsworth,  
1673 T. N.: 2016. Climate-growth relationships along a black spruce topose-quence in  
1674 interior Alaska, *Arctic, Antarctic, and Alpine Research*, 48,637-652, 2016.
- 1675  
1676 Wu, J., Roulet, N. T., Sagerfors, J., Nilsson, M. B.: Simulation of six years of carbon  
1677 fluxes for a sedge-dominated oligotrophic minerogenic peatland in Northern Sweden  
1678 using the McGill Wetland Model (MWM), *J. Geophys. Res. -Biogeosciences*,  
1679 [doi:10.1002/jgrg.20045](https://doi.org/10.1002/jgrg.20045), 2013.
- 1680 Wu, Y. and Blodau, C.: PEATBOG: a biogeochemical model for analyzing coupled  
1681 carbon and nitrogen dynamics in northern peatlands, *Geosci. Model Dev.*, 6, 1173-  
1682 1207, [doi:10.5194/gmd-6-1173-2013](https://doi.org/10.5194/gmd-6-1173-2013), 2013.
- 1683 Wu, J. and Roulet, N. T.: Climate change reduces the capacity of northern peatlands to  
1684 absorb the atmospheric carbon dioxide: The different responses of bogs and fens,  
1685 *Global Biogeochem. Cycles*, [doi.org/10.1002/2014GB004845](https://doi.org/10.1002/2014GB004845), 2014.
- 1686 Wu, Y., Verseghy, D. L., and Melton, J. R.: Integrating peatlands into the coupled  
1687 Canadian Land Surface Scheme (CLASS) v3.6 and the Canadian Terrestrial  
1688 Ecosystem Model (CTEM) v2.0, *Geosci. Model Dev.*, 9, 2639-2663,  
1689 [doi:10.5194/gmd-9-2639-2016](https://doi.org/10.5194/gmd-9-2639-2016), 2016.
- 1690 Yang, X., Ricciuto, D. M., Thornton, P. E., Shi, X., Xu, M., Hoffman, F., Norby R. J.:  
1691 The effects of phosphorus cycle dynamics on carbon sources and sinks in the Amazon  
1692 region: a modeling study using ELM v1, *J. Geophys. Res.-Biogeo*, 124,  
1693 <https://doi.org/10.1029/2019JG005082>, 2019.
- 1694 Yu, Z., Loisel, J., Brosseau, D. P., Beilman, D. W., and Hunt, S.J.: Global peatland  
1695 dynamics since the Last Glacial Maximum, *Geophys. Res. Lett.*, 37, L13402,  
1696 [doi:10.1029/2010GL043584](https://doi.org/10.1029/2010GL043584), 2010.



- 1697 Yurova, A., Wolf, A., Sagerfors, J., and Nilsson, M.: Variations in net ecosystem  
1698 exchange of carbon dioxide in a boreal mire: Modeling mechanisms linked to water  
1699 table position, *J. Geophys. Res.-Biogeo.*, 112, G02025, doi:10.1029/2006JG000342,  
1700 2007
- 1701 Zhang, W. X., Miller, P. A., Smith, B., Wania, R., Koenigk, T., and Doscher, R.: Tundra  
1702 shrubification and tree-line advance amplify arctic climate warming: results from an  
1703 individual- based dynamic vegetation model, *Environ. Res. Lett.*, 8, 034023,  
1704 <https://doi.org/10.1088/1748-9326/8/3/034023>, 2013.
- 1705 Zhuang, Q., Melillo, J.M., Sarofim, M.C., Kicklighter, D.W., McGuire, A.D., Felzer,  
1706 B.S., Sokolov, A., Prinn, R.G., Steudler, P.A., and Hu, S.: CO<sub>2</sub> and CH<sub>4</sub> exchanges  
1707 between land ecosystems and the atmosphere in northern high latitudes over the 21st  
1708 century, *Geophys. Res. Lett.*, 33, L17403, doi:10.1029/2006GL026972, 2006.  
1709  
1710

